Influence of substitution of water by organic solvents in amine solutions on absorption of CO_2

Monica Garcia [a], *Hanna K. Knuutila* [c], *Ugochukwu Edwin Aronu* [b], *Sai Gu* [a]*.

[a] Department of Chemical and Process Engineering, Faculty of Engineering and Physical Sciences, University of Surrey, Guildford, Surrey, UK. GU2 7XH

[b] Sustainable Energy Technology Sector, SINTEF Materials and Chemistry, Trondheim, Norway, NO-7465

[c] Department of Chemical Engineering, Norwegian University of Science and Technology (NTNU), Trondheim, Norway, Sem Saeland Vei 4, NO-7045.

* **Corresponding authors**: Prof Sai Gu, sai.gu@surrey.ac.uk

KEYWORDS CO_2 Capture; MEA; organic solvents; kinetics; mass transfer; Stirred Cell

ABSTRACT

Aqueous amine solutions are the most used solvents for chemical absorption of CO_2. Substituting part of the water by organic solvents in aqueous amine solutions aims to take advantage of the lower partial pressure and higher CO_2 solubility. In this work, the influence of four organic solvents on solution density, viscosity, N_2O solubility and absorption kinetics are studied. The organic solvents, Monoethylene Glycol (MEG), Diethylene Glycol (DEG), Triethylene Glycol (TEG) and CARBITOL, are blended with two amine solutions: MEA and DEEA-MAPA blend. The results show that the addition of organic solvents increases the density and viscosity. Furthermore, the N_2O solubility, used to estimate the physical solubility of CO_2 into a reactive system, increases when part of the water is substituted with an organic solvent. The kinetic experiments with a double stirred cell showed that in case of aqueous 5M MEA, the substitution of part of the water increases both the mass transfer and kinetic coefficients of the CO_2, whereas the substitution in the 3M DEEA+ 2M MAPA solution was not that favorable and only the substitution of MEG showed enhancement on the mass transfer and kinetic coefficients over the whole temperature range studied. The results can be partly explained by the changes in viscosity and N_2O solubility in the different systems, since the viscosity of the MEA organic solvent blends is lower compared to that of DEEA+MAPA blends and have less negative influence on the kinetics. At the same time the increase of N_2O solubility in the MEA blends is much higher than in DEEA+MAPA blends, resulting in more CO_2 available to react. Finally, the kinetic coefficients results are discussed together with dielectric constant of the dilution media to gain more insight.

1. INTRODUCTION

The global population is expected to continue growing from 7 to 9 billion by 2050, which will be linked to an increase of energy demand and emissions. Specifically, anthropogenic CO_2 emissions, considered the principal cause of global warming, will increase significantly. In 2014, emissions reached 36.6 Gt of CO_2 while cumulative emissions were more than 2000 Gt, shared between atmosphere, ocean and land [1].

One solution to decrease emissions is to focus efforts directly on the production points, the power plants. The main proposed technologies for decreasing or eliminating CO_2 emissions are pre-combustion, oxyfuel and post-combustion. Unlike pre-combustion and oxycombustion, which both require changes to process configuration, post-combustion takes place after the combustion, and so can be used for retrofitting, in addition to upgrades to ensure acceptable net efficiency.

Chemical absorption is considered the most feasible route for post-combustion at industrial applications such as power plants [2]. This technology is based on the use of a solvent solution that reacts with the CO_2 contained in the fluegas, separating it from the gas stream. After this step, which takes place in the absorber, the absorption reaction is reversed in the stripper by heating the solution. The stripping process produces the regenerated solvent solution to be reused in the absorber and a CO_2 stream that can be compressed and stored. The main weakness of the chemical absorption process is the high energy required for the solvent regeneration.

Monoethanolamine (MEA), a primary amine, is to date the most used solvent due to its high reactivity and economic performance. However, two major drawbacks of MEA are its high energy requirement during the solvent regeneration and problems related to corrosion. To reduce the energy requirements, several blends have been proposed in the literature, often being mixtures of

primary amines with tertiary amines [3,4]. The ideal solvent for chemical absorption would have a high reaction rate with respect to CO_2, low regeneration costs (low energy requirement), high absorption capacity, high thermal stability, low environmental impact and obviously low solvent cost [5].

A tertiary amine, N,N-dyetilethanolamine (DEEA), captures in aqueous solution a higher amount of CO_2 than MEA (mol CO_2 /mol amine) and has lower regeneration costs [1]. However, the absorption rate is lower than that of primary amines and the use of promoters is needed. A di-amine, N-methyl-1,3-propane-diamine (MAPA), which contains one primary amine group and one secondary amine group, has 15 times higher kinetic coefficients than those of MEA, twice those of Piperazine (PZ), eight times higher than 2-(2-amino-ethyl-amino)ethanol (AEEA) [2] and can be used as promoter in tertiary amine solutions. Monteiro et al. [3] studied the kinetics of the unloaded system DEEA+MAPA at different molarities for the families of 1M and 2M MAPA. Their results showed that the family of 2M MAPA + DEEA had higher mass transfer and kinetic coefficients than the family of 1M MAPA + DEEA, in case of unloaded solutions; the higher the content of MAPA, the higher the mass transfer and kinetic coefficients. The kinetic coefficient (k_{obs}) of 3M DEEA+ 2M MAPA was on average 87% higher than 2M MAPA between 298 and 333K. This increase of k_{obs} was due to DEEA, which promotes the hydrolysis of CO_2. However, the enhancement by DEEA is not very concentration dependent and 2M MAPA+2M DEEA showed similar behavior to 2M MAPA+3M DEEA.

During the chemical absorption of CO_2 into reactive components, physical absorption limits the available CO_2 for the chemical reactions. The substitution of water by organic solvents in amine solutions can be used to increase the physical solubility of CO_2 in the solution and decrease regeneration costs [4] due to changes in vapor-liquid equilibrium behavior and reduced heat

capacity [6]. Also, at high CO_2 pressure, existing physical solvents have shown high loading capacity and high selectivity between CO_2 and H_2S [8]. Moreover, the absorption kinetics might be improved by increasing the availability of CO_2 in the liquid phase for chemical absorption. However, organic solvents are usually more viscous than amines and consequently, that could influence negatively on the absorption kinetics, pumping costs and heat exchanger performance.

This paper studies the kinetics of unloaded blends of 30wt.-%MEA- 35wt.-% organic solvent-35wt.-%H_2O and 39.3wt.-% DEEA- 19.1wt.-%MAPA-21.3wt.-%H_2O-21.3wt.-% organic solvent. The organic solvents selected in this work are Monoethylene glycol (MEG), Diethylene Glycol (DEG), Triethylene Glycol (TEG) and CARBITOL.). The mass transfer of CO_2 absorption is measured from 303 to 353 K with a Double Stirred Cell apparatus (DSC). Furthermore, density, viscosity and physical solubility of N_2O for the studied blends were measured from 298 to 353K. Based on the experimental results, this paper discusses the advantages proposed in the literature: the increase on physical solubility of CO_2, density and viscosity and changes on mass transfer and kinetic coefficients. This study includes a discussion on the dependency of kinetic coefficients on physical properties and dielectric constants of the dilution media.

2. AVAILABLE LITERATURE DATA

Several literature reviews of the kinetics of MEA have been published over the years and will not be presented here [5–7]. Similarly an overview of the kinetic data for aqueous DEEA and MAPA solutions can be found elsewhere [3].

Table 1 Blends of organic solvents and amines reported in the literature

Reference	Temperature (K)	Blend*	Data
[8]	303-353	TEG+MEA	CO_2 solubility
[9]	333	PEG+MEG+MEA+H_2O	CO_2 Solubility
[4]	223-293	Methanol/ Ethanol/ THFS/ BA/ MEG/ DEG/ TEG/ PEG/ DPG/ 1,4 BUG/ 1,3 BUG / 2,3 BUG/ MEMMEG/ MPEDEG/ MEMPEG/ DMA/ DMF/ EA/ TG/ NMP/ Pyrrolidone/ Pyiperydone-2/ Formilmorpholine + MEA, Sulfonane +MEA+ H_2O	CO_2 Solubility; Heat consumption
[10]	313	NMP/ CARBITOL+MEA/DGA/TEG+H_2O+CO_2,	CO_2 Solubility; Mass transfer; Viscosity
[11]	303	MEG+MEA	CO_2 Solubility, Kinetics
[12]	323	DEG+DETA+PZ+H_2O	Mass transfer
[13]	300	MEA/DIPA+H_2O+ CARBITOL/ Methyl CARBITOL / CARBITOL Acetate/ DEG/DEG Dimethyl Ether/ Methoxy Triglycol/NMP/TEG / TEG Dimethyl ether/DMF	CO_2 Solubility; Absorption capacity; Qualitative kinetics and foaming
[14]	313	MDEA+Methanol	N_2O Solubility
[15]	293	MDEA+Ethanol	CO_2 Solubility
[16]	298	DEA+MEG	CO_2 Solubility; Equilibrium constant

*THFS= Tetrahydrofurfuril alcohol; BA= Benzyl alcohol; MEG=Monoethylenglycol DEG= diethylene glycol TEG= triethylene glycol PEG= poliethylene glycol DPG= Dipropylene glicol; 1,4-BUG= 1,4-Butylene glicol; 1,3-BUG= 1,3-Butylene glycol; 2,3-BUG= 2,3-Butylene glicol; MEMMEG= Monomethyl ether of ethylene glycol; MPEDEG = Monophenyl ether of diethylene glycol; MEMPEG= Monomethyl ether of propylene glycol; DMA= Dimethyl acetamide; DMF= Dimethyl formamide; EA= N, ethyl acetamide; TG= Tetraethyl glutaramide; NMP= N-methylpyrrolidone; CARBITOL= Diethylene glycol butyl ether; DETA= Diethylenetriamine; PZ= Piperazine; MDEA=methyl diethanolamine DEA= Diethanolamine; DMF= Dimethyl Formamide

Table 1 summarizes the available literature data for systems containing organic solvents. Organic solvents have been studied over the past six decades, and the separation of acidic constituents from gases using a blend containing a reactive component and glycols and/or alcohols was included in the patent already in 1952 [17]. Woertz [13] investigated more than 40 years ago the solubility of CO_2 in blends of aqueous amine and organic compounds. In his work, the presence of water was low (3-10wt.-% approximately) and the highest CO_2 removed per mole of amine was shown by 88wt.-%DMF+9wt.-%MEA+3wt.-%H_2O. Henni & Mather [14] and Kierzkowska-Pawlak & Zarzycki [15] focused their study in the addition of alcohols to MDEA solutions. Whereas, Aschenbrenner & Styring [18] highlighted the high solubility of CO_2 in organic solvents including glycerol and PEG200.

The family of glycols is commonly used in the dehydration process within the gas industry to reach acceptable concentrations of water and impurities in the gas transported. Usually, one glycol compound (MEG, DEG or TEG) is used although blends have also been proposed in the literature. TEG has been the most used in the gas sector due to its price, superior dew point depression, operating cost, and operation reliability.

The solubility of CO_2 in pure DEG was measured in the work of Jou et al. [19]. Tan et al.[8] studied the VLE of the CO_2 absorption in pure TEG and loaded MEA+TEG solutions from 303 to 353 K

at low concentrations of MEA, from 0.1 to 0.5 M. They reported that the physical solubility of CO_2 in pure TEG is slightly lower than this in pure DEG. At low MEA concentrations and low temperature, the physical solvent plays an important role in the CO_2 solubility and the presence of TEG becomes more important. Furthermore, Song et al. [9] reported the influence of the addition of 15.3 and 42.3wt.-% of organic solvents, MEG and Poliethylene Glycol (PEG), to 15.3wt.-% aqueous MEA solutions. The results showed that the physical solubility of CO_2 increased with higher additions of organic solvents and both, PEG and MEG, exhibited similar results. Likewise, Leites [4] reported increased physical solubility of CO_2 into hybrid solvents of MEA with glycols and esters of glycols at 293K. The mixtures contained 2.5 M MEA and were non-aqueous solutions. The physical solubility of CO_2 followed a descendent order as MEG>TEG>DEG. Moreover, he also studied the heat consumption during regeneration of mixtures of MEA with organic solvents in a pilot. N-Methylpyrrolidone (NMP) showed the lowest energy consumption, followed by Tetrahydrofurfuril alcohol (THFS) and MEG. However, the percentage of organic solvents and MEA varied between 68-74wt.-% and between 11 to 21wt.-%, respectively, making it difficult to compare the performance of the tested hybrid solvents.

Jiru & Eimer [11] reported that blending MEG and MEA increased the absorption rate of CO_2 at 303K compared to aqueous MEA solutions. Similarly, Yuan & Rochelle [10] reported the addition of N-methyl-2-pyrrolidone (NMP) and CARBITOL to loaded aqueous 7mMEA solutions, with a mass proportion of 1:3 and 3:1 for NMP/CARBITOL: Water. At low CO_2 loadings (approximately up to 0.4 mol CO_2/mol MEA), their results showed that both organic solvents, NMP and CARBITOL, increased the mass transfer and it was higher at higher NMP/ CARBITOL ratios. In contrast to these results, Yu & Tan [12] reported that DEG had a negative effect on the mass transfer coefficients in blends of 37wt.-% DEG (in approximately 2:1 for

DEG:H_2O mass proportion) with aqueous DETA (Diethylenetriamine)+PZ (piperazine) blend at 323 K in a rotating packed bed. The results also showed that the energy invested for solvent regeneration in presence of DEG decreased by 21.5% in comparison to the original blend of DETA+PZ+H_2O.

3. ABSORPTION OF CO_2 IN AMINE SOLUTIONS

3.1 MEA Solutions

MEA is a primary amine which reacts directly with CO_2 and forms carbamate (Equation 1). In aqueous MEA solutions, simultaneously, the reactions of the dissociation of MEA and hydration of CO_2 also take place, as described in Equations 2-3. The Equation 3, however, is negligible in unloaded MEA solutions due to the low concentration of OH^- [3].

$$\boldsymbol{C\,O_2 + MEA + H_2O \leftrightarrow MEACOO^-\ + H_3O^+} \quad (1)$$

$$\boldsymbol{MEA + H_3O^+ \leftrightarrow MEAH^+ + H_2O} \quad (2)$$

$$\boldsymbol{CO_2 + OH^- \leftrightarrow HCO_3^-} \quad (3)$$

There are two common theories to describe the reaction: the zwitterion mechanism and the termolecular mechanism Crooks & Donnellan [20]. The zwitterion mechanism, proposed initially by Caplow [21], was used in this work. This mechanism was is based on the creation of an intermediate (Equations 4-5), where the reaction rate can be described as Equation 6.

$$MEA + CO_2 \overset{k_3,k_{-3}}{\longleftrightarrow} MEA^+COO^- \quad (4)$$

$$MEA^+COO^- + B \overset{k_4}{\rightarrow} MEACOO^- + B^+ \quad (5)$$

$$r_{CO_2} = \frac{k_2[CO_2][AMINE]}{1+\frac{k_{-3}}{k_4[B]}} \quad (6)$$

In the Equations, the base, B, can be both water and MEA and the zwitterion reaches a pseudo-equilibrium condition. Since the reverse reaction, k_{-3} , in Equation 4 is much slower than the loss of the proton of the zwitterion (Equation 6), $\frac{k_{-3}}{k_4[B]}$ is considerably smaller than 1 and can be negligible. Thus, the calculation of the reaction rate of CO_2 becomes first order for MEA and second order for the overall reaction as shown in Equation 7.

$$r_{CO_2} = k[AMINE]^n[CO_2] = k_{obs}[CO_2] \quad (7)$$

3.2 DEEA+ MAPA solutions

MAPA, is a primary amine that reacts directly with CO_2 and has two amine groups, which results in a higher absorption capacity of CO_2 than that in MEA. Its reaction with CO_2 produces two stable carbamates (Equation 8) that become bicarbamate in the presence of a base (Equation 9). Although MAPA has the strongest absorption effect in the blends DEEA+MAPA, the addition of DEEA to MAPA solutions increases the observed kinetic coefficients [3]. DEEA is a tertiary amine that can be obtained from renewable sources [22] and does not react with CO_2 (pH <13) but promotes the hydrolysis of CO_2 (Equation 10). In addition, DEEA presents a low energy requirements for its regeneration. Further reviews are included in Monteiro et al. [23,24] and Garcia et al. [25].

$$MAPA + CO_2 \overset{k_2,k_{-2}}{\longleftrightarrow} MAPA^+COO^- \quad (8)$$

$$MAPA^+COO^- + B \overset{k_5}{\longrightarrow} MAPACOO^- + B^+ \quad (9)$$

$$DEEAH^+ + \mathrm{HC}O_3^- \leftrightarrow DEEA + H_2O + CO_2\,H_3O^+ \quad (10)$$

The hydrolysis of CO_2 (Equation 3) is a slow conversion compared to the reaction of CO_2 with MAPA (Equation 8) [3,26]. In addition, as mentioned before, the Equation 3 is limited by the concentration of the hydroxyl ion in the solution. Consequently, the CO_2 absorption is mainly based on the formation of the carbamates of MAPA. As seen in Garcia et al. [26], based on the zwitterion mechanism and the pseudo-equilibrium condition proposed by Danckwerts [27], the reaction rate of the absorption of CO_2 in MAPA can be described similarly to that of MEA in Equations 6 and 7 when it is assumed that .

- the reverse of the absorption of CO_2 in MAPA is much slower than the conversion of the zwitterion to carbamate
- And k_{-3} and k_4 are replaced with k_{-2} and k_5 in Equations 8 and 9.

Here n is the kinetic order of the reaction over the concentration of MAPA. Monteiro et al. [28] measured the observed kinetic coefficients of the absorption of CO_2 into MAPA solutions at various concentrations, from 1 to 5M. From their wok, the kinetic order n can be extracted through the slope of the logarithmic representation of the kinetic coefficients over MAPA concentration. The slope obtained was 0.5 (R^2=0.9983), and hence the order of the reaction n with respect MAPA in aqueous solutions can be determined as unity, as done in Sada et al. [29].However, as included in in Sada et al. [29], the reaction order changes based on the solution media because the reaction is influenced by an electrostatic interaction. That means that for solutions containing organic solvents, the order n with respect the primary amine, MAPA or MEA, is expected to increase. This increase has been extrapolated based on the results of the primary di-amine ethylenediamine (EDA) in Sada et al. [29], as function of the molar concentration of the organic solvent. Then, the order n was determined as 1.13, 1.08, 1.06 and 1.07 for the solution media being MEG+H_2O, DEG+H_2O, TEG+H_2O and CARBITOL+H_2O respectively.

4. EXPERIMENTAL WORK

4.1 Chemicals

In addition to the chemicals in the Table 2, de-ionised water was used for solution preparation. The solutions were prepared by weight without further purification of the chemicals received. Amine concentrations were checked by titration before and after kinetic experiments. The chemical structures of the components are included in Table 3 and the blends studied in this work are shown in Table 4.

Table 2 Chemicals used in this work

Product	**CAS number**	**Purity**	**Supplier**
MEA	141-43-5	99%	Sigma-Aldrich
MAPA	6291-84-5	97%	Sigma-Aldrich
DEEA	100-37-8	99.5%	Sigma-Aldrich
CO_2	124-38-9	100%	Aga
N_2O	10024-97-2	100%	Aga
N_2	7727-37-9	100%	Aga
MEG	107-21-1	99%	Sigma-Aldrich
DEG	111-46-6	99%	Sigma-Aldrich
TEG	112-27-6	99%	Sigma-Aldrich
CARBITOL	111-90-0	99%	Sigma-Aldrich

MEA: Monoethanolamine; MAPA: N-methyl-1,3-propane-diamine; DEEA: Diethylethanolamine; CO_2: Carbon dioxide; N_2O: Nitrous oxide; N_2: Nitrogen; MMAPEG: Monoethylene Glycol; DEG: Diethylene Glycol; TEG: Triethylene Glycol; CARBITOL: Diethylene glycol butyl ether

Table 3 Chemical structures of (from left to right and from top to bottom) MEA, MAPA, DEEA, MEG, DEG, TEG, CARBITOL

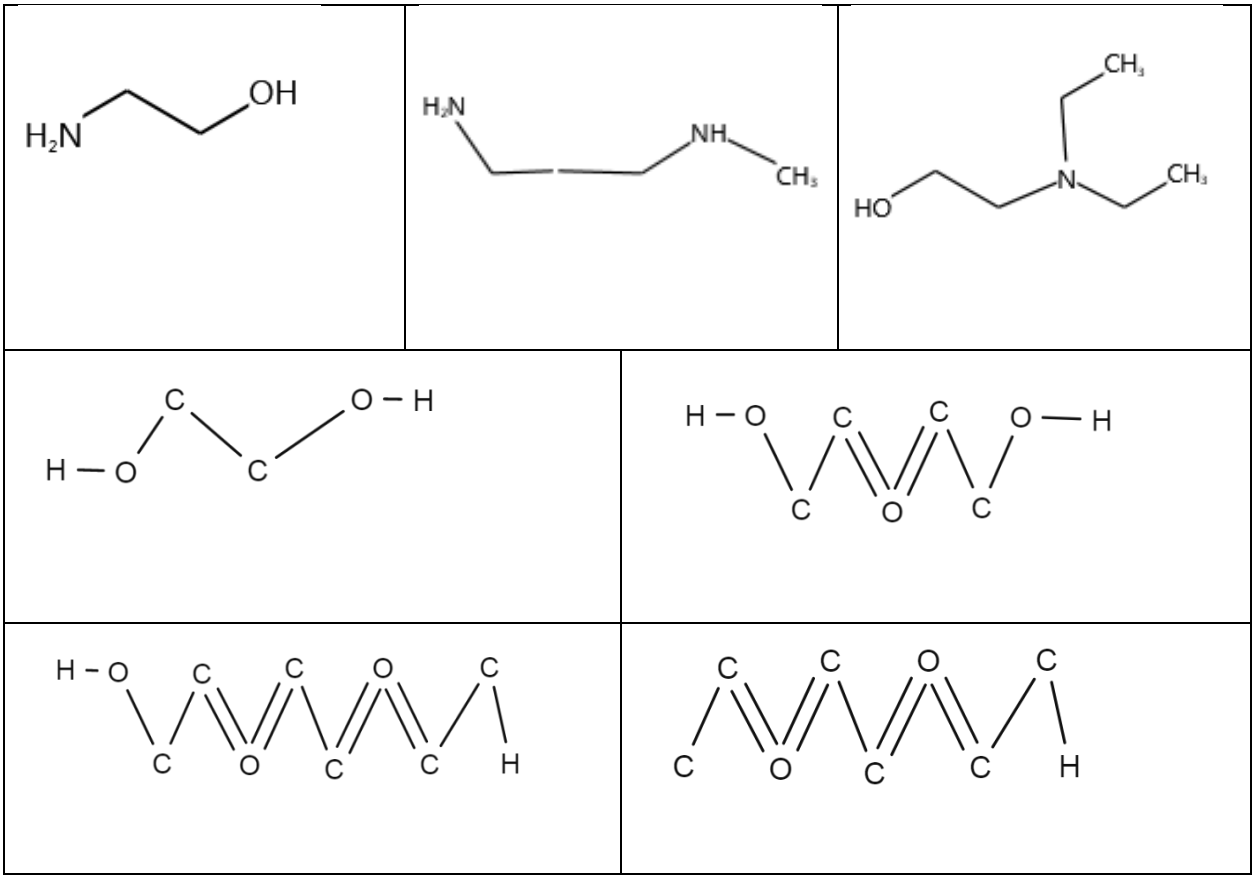

Table 4 Molar concentrations of the blends studied in this work.

Short name	DEEA (mol/L)	MAPA (mol/L)	MEA (mol/L)	Organic solvent (mol/L)	DEEA mol%	MAPA mol%	MEA mol%	Organic solvent mol%	Water mol%	Organic Solvent
3D2M	3	2		0	11.2	7.5		0.0	81.3	
3D2M+ MEG	3	2		3.43	15.8	10.5		16.6	57.1	MEG
3D2M+ DEG	3	2		2	17.0	11.2		10.4	61.4	DEG
3D2M+ TEG	3	2		1.41	17.5	11.6		7.6	63.3	TEG
3D2M+ CARBITOL	3	2		1.59	17.3	11.5		8.4	62.7	CARBITOL
5MEA			5	0			11.2	0.0	88.8	
5MEA+ MEG			5	5.63			16.4	18.8	64.8	MEG
5MEA+ DEG			5	2.18			17.8	11.9	70.3	DEG
5MEA+ TEG			5	2.33			18.4	8.7	72.8	TEG
5MEA+ CARBITOL			5	2.6			18.2	9.7	72.1	CARBITOL

Table 5 Mass concentrations of the blends studied in this work.

Short name	DEEA (mol/L)	MAPA (mol/L)	Organic solvent (mol/L)	DEEA (wt%)	MAPA (wt%)	Organic solvent (wt%)	Organic Solvent
3D2M	3	2	0	38.3	19.1	0	-
3D2M+MEG	3	2	3.43	38.3	19.1	21.3	MEG
3D2M+DEG	3	2	2	38.3	19.1	21.3	DEG
3D2M+TEG	3	2	1.41	38.3	19.1	21.3	TEG
3D2M+CARBITOL	3	2	1.59	38.3	19.1	21.3	CARBITOL

Short name	MEA (mol/L)	Organic solvent (mol/L)	MEA (wt%)	Organic solvent (wt%)	Organic Solvent
5MEA	5	0	30	0	-
5MEA+MEG	5	5.63	30	35	MEG
5MEA+DEG	5	2.18	30	35	DEG
5MEA+TEG	5	2.33	30	35	TEG
5MEA+CARBITOL	5	2.60	30	35	CARBITOL

4.2 Densitometer

Densities were measured with an Anton Paar DMA 4500 M densitometer, with an accuracy of ±0.00005g/cm^3 in density and 0.03ºC in temperature [30] . The apparatus used a Xsampler 452 H heating attachment to control the temperature with variability of 0.01 ºC. Tube samples were filled

with 10 ml of solutions and washed with water and acetone between the experiments, followed by air drying. The method and the equipment were the same as those used in Pinto et al. and Gondal et al.[31,32]. For each sample two measurements were taken, and the average is reported in this work. Several samples of water were placed in between the samples in order to check the uncertainty. The AARD, calculated using Equation 13, for the water samples was 0.008%.

$$AARD(\%) = \frac{|X_{this\ work} - X_{literature}|}{X_{literature}} \cdot 100 \quad (13)$$

4.3 Rheometer

An Anton Paar MCR 100 rheometer with a double gap measuring cell (DG-26.7) was used to measure the dynamic viscosity. The setup and the method were the same as in Aronu et al. [30], with an accuracy of 0.1%. The temperature was controlled using a water bath and maintained constant for a minimum of 180 s before starting the measurement. The gear was calibrated every day before starting the measurements with deviations below ±5% of oscillation.

4 ml of sample was used for each test and the dynamic viscosities were calculated based on the slope between the shear rate and shear stress. The reproducibility of the measurements was checked prior the measurement using the standard S60. The average deviation error (AARD, Equation 13) for the standard S60 was 0.8%.

4.4 Physical solubility

The measurements of physical solubility of N_2O were performed from 303 to 353 K using an apparatus and procedure used in several works [28,32]. The apparatus, shown in Table 6, contains

a glass reactor connected to a stainless vessel for N_2O. The glass reactor was agitated with a stirrer. The temperature of the jacketed reactor was controlled by using ethylene glycol as a heating medium in a heating bath. The top of the jacketed reactor was insulated to avoid thermal losses.

The experiments were carried out in batches and the reactor was cleaned between the experiments with hot water, deionized water and acetone. The solvent was added into the glass reactor by suction and the amount added was measured by weight difference. The stainless vessel was charged with N_2O and closed. The glass reactor was fed with N_2O from the stainless steel vessel when needed. The temperatures and pressures in the vessel and reactor were logged.

The solution was stirred and heated by steps to record the vapour

pressures of the solvent. The conditions were considered stable when pressures in the reactor changed in less than 5 mbar and temperature of the liquid changed in average less than 0.0125 ºC during 10 min. The equilibrium was reached when additionally, differences between liquid and gas temperatures were lower than 0.2 °C. Then, N_2O was injected and the system was allowed to reach equilibrium (stabilization of both pressures and temperatures in the reactor). The amount of N_2O fed from the vessel was calculated by mass balance using Peng-Robinson Equation of state. The physical solubility of N_2O measured was then used to calculate the physical solubility of CO_2 into the reactive solution using Equations 14-15 [33]:

$$H_{CO_2-sol} = \frac{H_{N_2O-sol}}{R_H} \quad (14)$$

Where R_H is a correlation factor between the solubility of the two gases, CO_2 and N_2O, in water according to the Equation 15 [33]:

$$R_H = \frac{H^{\infty}_{CO_2}}{H^{\infty}_{N_2O}} \quad (15)$$

Table 6 Characteristics of the solubility apparatus and double stirred cell (DSC)

Parameter	Units	Solubility	DSC
Glass Reactor Volume (V_{VLE}, V)	L	1.0112	0.586
Stainless vessel Volume (V_{vessel})	L	1.0362	-
Solvent volumen ($V_{solvent}$)	L	0.4-0.5	0.32-0.35
Stirrer Speed (approx.)	rpm	1000	
Interfacial area	m^2		3.15E-03
Liquid stirrer diameter (Ø)	m	0.035	0.035
Gas stirrer diameter ($Ø_G$)	m	-	0.035

4.5 Double Stirred Cell

The mass transfer and kinetics coefficients (k'_G and k_{obs}) were measured with a double stirred cell (Figure 2). The cell, manufactured by Parr® Instrument Company, had an inner diameter of 6.35 cm. The main characteristics are included in Table 6.

An external thermal jacket was used to heat the system. It also acted as insulator to avoid thermal losses. In order to increase the insulation of the stirred cell, some glass fiber was placed on the top. The stirred cell had two stirrers, one for the gas phase and another one for the liquid phase. The reactor had an internal height of 20.3cm and internal diameter of 6.35cm, with two stirrers of diameter 3.51cm. The reactor can be operated up to 350ºC and 140bar. The two stirrers driven by two independent shafts were mounted in the liquid and gas phase and can be stirred at speeds 0-1200 rpm and 0- 800rpm respectively. In order to avoid vortex and obtain a flat interface, a Teflon cylinder baffle was installed inside the stirred cell. It was made of one piece formed by three circumferences (at the top, at the middle and on the bottom), with same diameter than the reactor inner diameter, joined with four rectangular pieces along the height of the baffle.

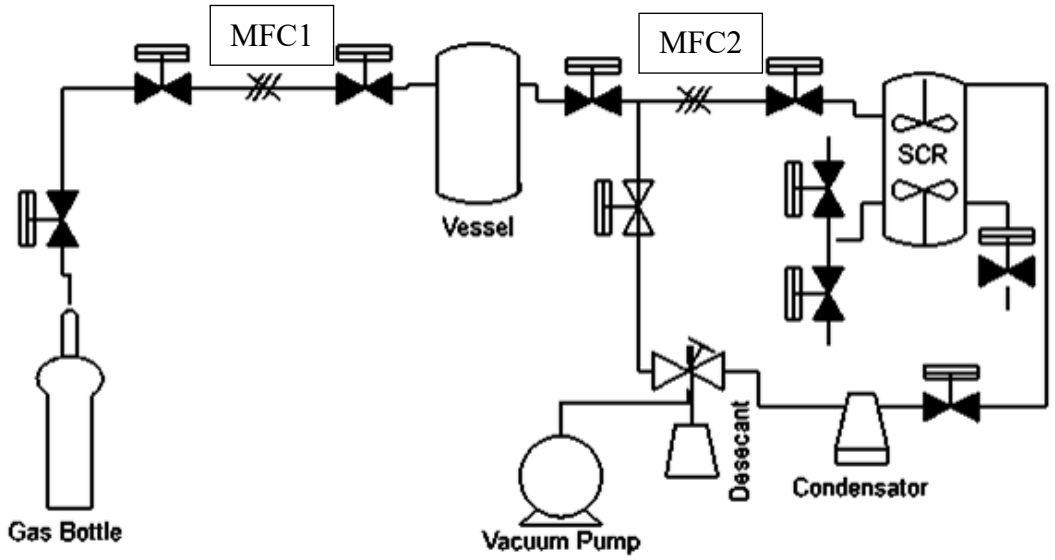

Figure 1 Double Stirred Cell (DSC, also called Stirred Cell Reactor, SCR) configuration used in this work (MFC= Mass Flow Controller; SCR= Double Stirred Cell Reactor).

The system was checked to be leak tight. The amount of gas added was controlled with digital mass flow meters (Figure 1) (Bronkhorst ®High Tech) calibrated with CO_2. The liquid was injected manually and the amount added was measured by weight difference (±0.01 g). The stirred cell was connected to a controller allowing to set stirrer speed, temperatures and heating rate. The reactor was installed with two J-type thermocouples with accuracy ±1ºC in the liquid and gas phase. The reactor pressure was monitored with a Druck Pressure transmitter PTX 7517-1 with uncertainty ± 0.1% (2 bar a) of full scale.

A small amount of CO_2 ($5 \cdot 10^{-5}$-$2 \cdot 10^{-4}$ moles of CO_2) was injected in a short time (max 4s). The moles of CO_2 injected were calculated by the pressure difference in the CO_2 tank and the Peng-Robinson equation of state. The amount should be high enough to cause a noticeable change of

the total pressure but without causing large changes on loading. All experiments were carried out with similar P_{CO_2} (3-24 kPa) as previously reported by Littel et al.[34] and Monteiro et al.[3]. After the experiment, the solution was analyzed by titration to check that the amine concentration was maintained constant. After each experiment, the CO_2 loading was analyzed using the wet-chemistry method described in Ma'mun et al[47] The loading found was below the limit of quantification. Luckily, the amount of injected CO_2 can be used to calculate the loading together with the analyzed amine concentration..

The experiments were carried out in batches, after which the reactor was cleaned with hot water and deionized water two times. The reactor was then dried with synthetic air for 1 hour to eliminate any rest of water, CO_2 and other gas and aqueous products after each experiment. In addition, the apparatus was dismantled, cleaned and dried carefully after all the measurements were taken for a specific blend and before testing the next one.

5. EXPERIMENTAL CONDITIONS AND DATA TREATMENT

5.1 Stirrer speed

As mentioned in Ying & Eimer [35], liquid stirrer speed can influence the kinetics measurement due to its influence in the gas-liquid surface. This assumption is based on Danckwerts theory, which describes the renewal of the gas-liquid layer on the interface during stirring [27], [36]. At very low velocity, stirring is not strong enough to renew the liquid surface. Consequently, that results in too low mass transfer and chemical reaction rates. On the other hand, too high velocity creates turbulences on the surface which creates a non-stable gas-liquid surface for the mass transfer and characterization of the mass transfer area becomes impossible. In this work, in order to find the stirrer speed region where the flux is independent of the stirring speed and allow the

treatment of the data based on pseudo first order condition, a study of the stirring conditions was done.

The liquid stirrer speed was varied from 30 to 130 rpm while the gas stirrer was maintained at 600 rpm to minimize the influence of the gas resistance. After creating a vacuum in the reactor, a known amount of water was added in the stirred cell and reactor was vacuumed one more time to remove air/gas that could be introduced in the reactor during liquid injection. The reactor was then heated to 303K (±0.2 K) and $5 \cdot 10^{-5}$-$2 \cdot 10^{-4}$ moles of CO_2 were injected in a time period of ~4s. The total pressure was recorded continuously while the temperature was logged and the stirrer velocities were kept constant. The partial pressure of CO_2 was calculated from the total pressure and the initial solution vapor pressure (P_{sol}), measured before the CO_2 injection (average of 100 seconds). The moles of CO_2 injected were calculated by the pressure difference and the Peng-Robinson equation of state. Variation of the stirring speed showed that the CO_2 absorption flux was independent of the stirring speed at 70-100rpm. Thus, the experiments were carried out at 70 rpm with repetitions at 100 rpm.

5.2 Treatment of kinetic data

For the treatment of kinetic data, the zwitterion mechanism was used together with the two-film theory. Additionally, the conditions of the experiments were suitable to consider the pseudo-first order regime.

Previous studies using the Double Stirred Cell apparatus included the pressure variation as main parameter to calculate the kinetic rate [11,35,37,38]. Based on the physical absorption and supported on the ideal gas law [38], for unloaded solutions, the molar transfer between gas and

liquid can be expressed as a function of the partial pressure of CO_2. Applying the two film theory [35], Equations 16 and 17 are obtained:

$$\frac{dn_{CO_2,g}}{dt} = \frac{V_G}{RT}\frac{dP_{CO_2}}{dt} = \frac{1}{\frac{1}{k_g}+\frac{H}{E\,k_L^{\circ}}}\,A\,P_{CO_2} \tag{16}$$

$$\frac{dn_{CO_2,L}}{dt} = k_G\,A\left(C_{CO_2}^{i}\right) = -\frac{dn_{CO_2,g}}{dt} \tag{17}$$

Where $C_{CO_2}^{i}\ is$ the increase of the concentrations of CO_2 in the interface, which can be expressed by the partial pressure of CO_2 and its Henry´s law constant; and k_L° is the physical mass transfer coefficient.

Re-arranging Equation 16 and the mass transfer coefficients, the temporal variation of the partial pressure of CO_2 can be expressed as

$$\frac{dP_{CO_2}}{dt} = \frac{RAT\,P_{CO_2}}{V_G\,(\frac{1}{k_g}+\frac{H}{E\,k_L^{\circ}})} = \frac{RAT\,P_{CO_2}}{V_G\,(\frac{1}{k_g}+\frac{1}{k'_G})} = \frac{RAT\,P_{CO_2}}{V_G\,K_G} \tag{18}$$

There are two models to estimate the mass transfer coefficient k'_G; derivative or integral [38]. In this work, the integral method is used. Taking into account that the gas resistance is neglected in Equation 18 because pure CO_2, is used [38], the equation becomes

$$\ln p = -\frac{RTA}{V_G H}\sqrt{k_{obs}\,D_{CO_2-sol}}\,t + \ln p_0 \tag{19}$$

A typical pressure curve is shown in Figure 3. Since only unloaded solutions were studied, the initial partial pressure of CO_2 ,p_0, is zero and k_{obs} can be calculated by

$$\boldsymbol{k_{obs}} = \left(\frac{-\frac{d\ln P_{CO_2}}{dt}\,H\,V_G}{RTA}\right)^2 \frac{1}{D_{CO_2-sol}} \tag{20}$$

Note that the kinetic constant k_{obs} contains the individual contributions of the species, as in Monteiro et al. [2] . Moreover, considering that the fast reaction only takes place in the reaction layer, the k'_G can also be calculated based on the assumption of pseudo-first order regime (Equation 21).

$$k_G^{'} = \frac{\sqrt{k_{obs}\, D_{CO_2-sol}}}{H} = \frac{-\frac{\mathrm{dln}\, P_{CO_2}}{\mathrm{dt}}\, V_G}{\mathrm{RTA}} \quad (21)$$

Where H is the Henry constant of CO_2 in the solution, T (K) is the temperature of the solvent, R is the gas constant, A is the area of the contact surface, $D_{i\text{-}sol}$ is the diffusion of the component i in the solution and V_G is the volume of the gas in the double stirred cell.

The calculated k, the second order kinetic constant, can be extracted from the observed kinetic constant, k_{obs} (Equation 20), where [Amine] is the concentration of primary amine in the solutions, MEA and MAPA.

$$k = \frac{k_{obs}}{[Amine]} \quad (22)$$

The pseudo-first order is reached if the amine volume is large enough to be constant over the reaction layer. The Hatta number (Ha) and E_{inf} (infinite reaction rate enhancement factor) gives an estimation on how fast is the reaction. Specifically, the pseudo first order is achieved when Ha>>5 and E_{inf}>>a. Hatta number (Ha) and infinite enhancement factor (E_{inf}) are calculated using Equations 23-25 :

$$Ha = \frac{\sqrt{k_{obs}\, D_{CO_2-sol}}}{k_L^{\circ}} \quad (23)$$

$$E_{inf} = 1 + \frac{D_{amine-sol} C_{amine}}{D_{CO_2-sol}\, C_{CO_2} \nu_{amine}} \quad (24)$$

$$k_L^{\circ} = \frac{Sh\, D_{CO_2-sol}}{\emptyset} \quad (25)$$

In Equations 25-27 Ø is the stirrer diameter; $D_{i\text{-}sol}$ is the diffusivity of the component i in the solution; C_i is the concentration of the specie i; μ is the viscosity of the solution; and ρ is the density of the solution. there are numerous correlations based on the Reynolds (Re) and Schmidt numbers (Sc) to calculate Sherwood number (Sh[35,38–40]. In this work, the correlation was obtained during reactor characterization and is shown below

$$Sh = 1.4513\, Re^{0.4367} Sc^{0.5} \quad (26)$$

Where Schmidt and Reynolds numbers were calculated from

$$Sc = \frac{D_{CO_2-sol}}{\rho\, \mu} \quad (27)$$

$$Re = \frac{\rho\, w \emptyset^2}{\mu} \quad (28)$$

In Equation 28 w is the liquid stirrer velocity.

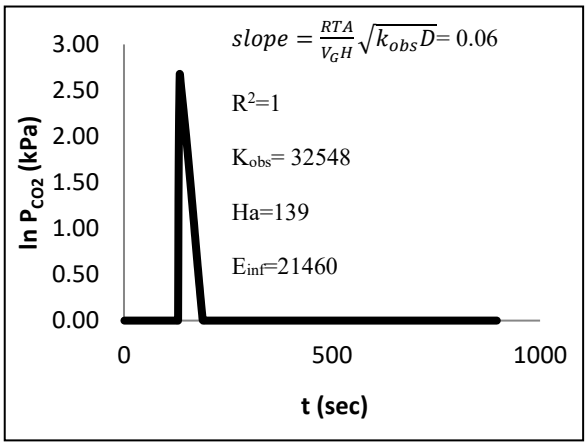

Figure 2 Example with 30% MEA at 303 K

5.3 Diffusivities

For the solutions studied in this work, the diffusivities were calculated based on the CO_2-H_2O analogy:

$$D_{Co2-sol=}D_{Co2-water}\left(\frac{\mu_{water}}{\mu_{solution}}\right)^{0.8} \quad (29)$$

The viscosity of water was extracted from the work of Korson et al. [41] and the viscosities of the blends were measured. The diffusivity of CO_2 in water was interpolated from Versteeg & Van Swaaij [42]. For the physical CO_2 solubility, the N_2O analogy shown in Equations 14-15 was used. The diffusion of the MEA in the 5M MEA solutions was calculated with correlation from literature [43]. The diffusivities calculated with those correlations are in relatively good agreement with other literature data with 11% deviation between diffusivities published by Ying & Eimer [44].

$$D_{amine-water} = 2.5\ 10^{-10}\left(\frac{M}{\rho}\right)^{-0.54} \quad (30)$$

$$D_{amine-sol} = D_{amine-water}\frac{T}{298}\left(\frac{\mu_{H_2O}}{\mu_{sol}}\right)^{0.6} \quad (31)$$

6. RESULTS AND DISCUSSION

In this section, the results from density, viscosity and, N_2O physical solubility are presented and discussed as well as the mass transfer and kinetics coefficients of the absorption of CO_2 into the blends. All measurements are shown in Tables A1-A15. Average Absolute Relative Deviation (%AARD) was calculated by Equation 13.

6.1 Density

Figure 3 shows the results for MEA blends, while Figure 4 shows the results for blends of 3D2M. The densities of both hybrid blends families, 5MEA+MEEG/DEG/TEG/CARBITOL and 3D2M+ MEG/DEG/TEG/CARBITOL, are compared in Figure 5.

As seen in Figure 3, the substitution of 50wt.-% of the water content in 5M MEA aqueous solutions by MEG, TEG or DEG has very similar influence on density, with MEG showing slightly lower densities. The same fact is seen in Figure 4 for 3D2M blended with MEG, TEG and DEG even though the absolute values for 3D2M blends are lower. For both amine systems the lowest densities are seen in the blends with CARBITOL. Figure 6 shows that the density of 5MEA is higher than 3D2M and the influence of the organic solvent added is larger in 5MEA solutions with a relative difference varying from 6 to 9% at 25 ºC.

The data also shows that, in the case of 5MEA, the influence of temperature on density is larger for 5MEA+CARBITOL than that in aqueous MEA. This is visible in Figure 4. The density of 5MEA+CARBITOL is higher than that of 5MEA at low temperatures, but at the highest temperature the density is the same. In the case of 3D2M blends, at 353 K, some differences are observed: 3D2M+MEG, which had higher density than 3D2M+DEG up to 340K, shows lower density at 353 K. Similarly, the density difference between 3D2M+DEG and 3D2M decreases with temperature whereas the density difference between 3D2M and 3D2M+CARBITOL increases as temperature increases.

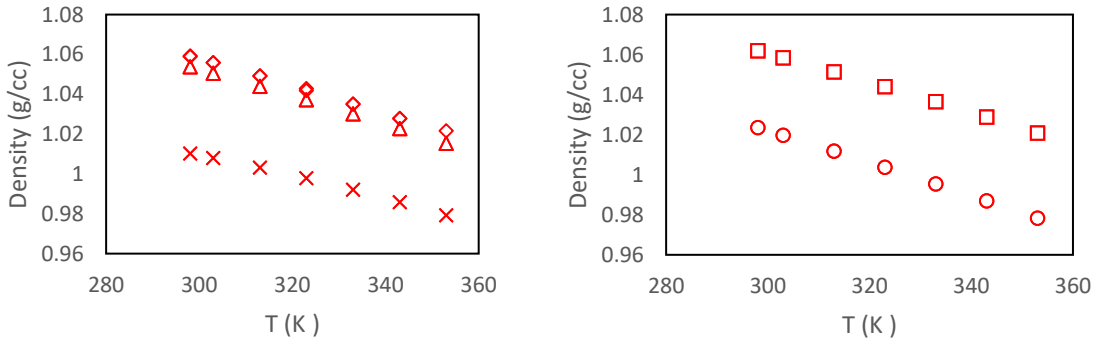

Figure 3 Densities (g/cc) measured in this work. (left) 5MEA (X), 5MEA+MEG (Δ), 5MEA+DEG (◊); 5MEA+TEG (□) and 5MEA+ CARBITOL (○).

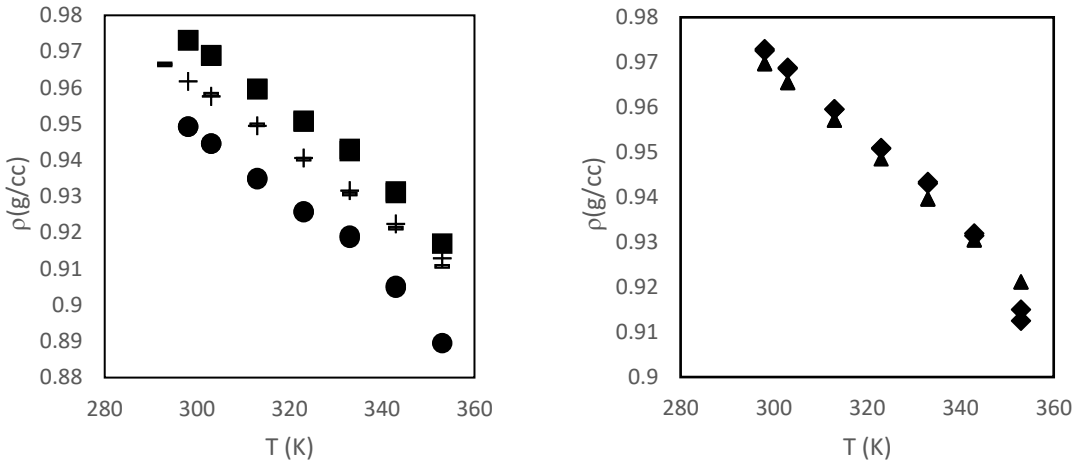

Figure 4 Densities, from 298 to 353K, of (Left) 3D2M, measured in Garcia et al. [26] (+), 3D2M+MEG (▲),3D2M+DEG (♦); 3D2M +TEG (■) and 3D2M + CARBITOL (●)

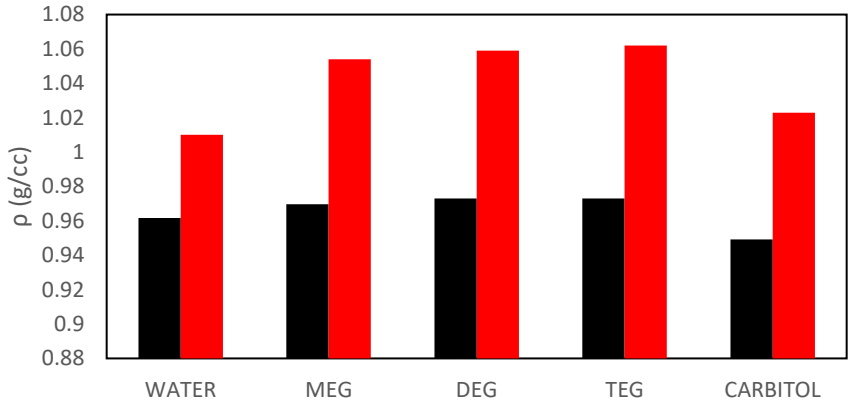

Figure 5 Density (g/cc) at 298K of 3D2M([26], and 3D2M+MEG/DEG/TEG/CARBITOL (black), compared to 5MEA+MEG/DEG/TEG/CARBITOL/WATER blends (red).

6.2 Viscosity

The value of viscosity influences the calculated value of the diffusivity of CO_2 into the solution, which consequently affects the calculated kinetic coefficients, k_{obs} and k (Equations 20 and 22). The viscosities of the blends considered in this study were measured from 298 to 353 K. The addition of organic solvents to the aqueous amine solutions studied in this work, increases the viscosity (Figure 6 and Figure 7). Figure 6 shows that the 5MEA solution exhibits the lowest

viscosity. 5MEA+TEG has the highest viscosity in the temperature range studied, almost three times the value of that of 5MEA at high temperatures, and four times at 298K. The viscosities of solutions containing DEG, CARBITOL and MEG are in between those 5MEA+TEG and 5MEA, with a 30-40% (from high to low temperature) lower viscosities compared to 5MEA+TEG. As seen in Figure 6, the differences in viscosities between the DEG, CARBITOL and MEG blends decrease as temperature increases. Similar behavior is observed in 3D2M solutions as shown in **Figure 7**. However, as illustrated in Figure 8, at 298K, the 3D2M systems have a higher dynamic viscosity than 5M MEA systems. Furthermore, the average viscosity from 298 to 353K of 3D2M is 3.2 times higher than that of 5MEA, while the average viscosity from 298 to 353K of 3D2M+MEG is 2.2 times higher than 5MEA+MEG. The lowest difference is observed in the blends containing CARBITOL, where the average viscosity of 3D2M+CARBITOL was only 30% higher than that of 5MEA+CARBITOL.

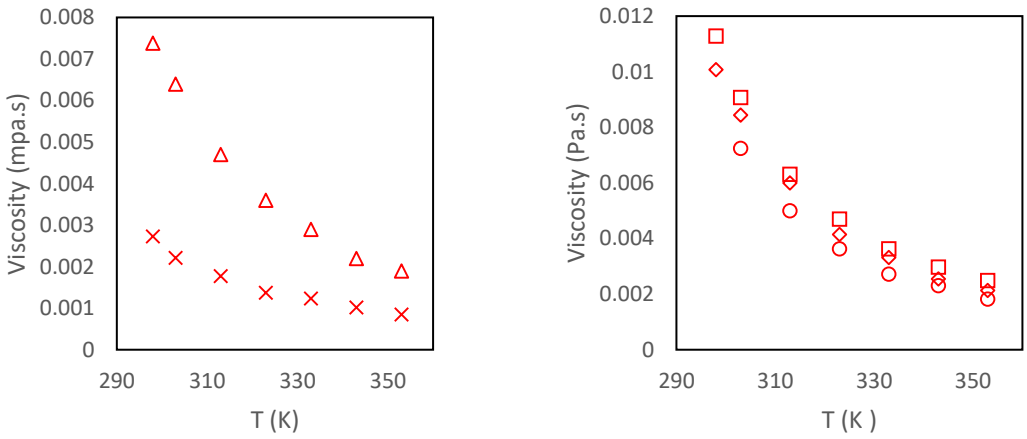

Figure 6 Dynamic viscosities (Pa s) (left) of aqueous solutions of 5MEA (X), 5MEA+MEG (Δ), 5MEA+DEG (◊); 5MEA+TEG (□) and 5MEA+ CARBITOL (○).

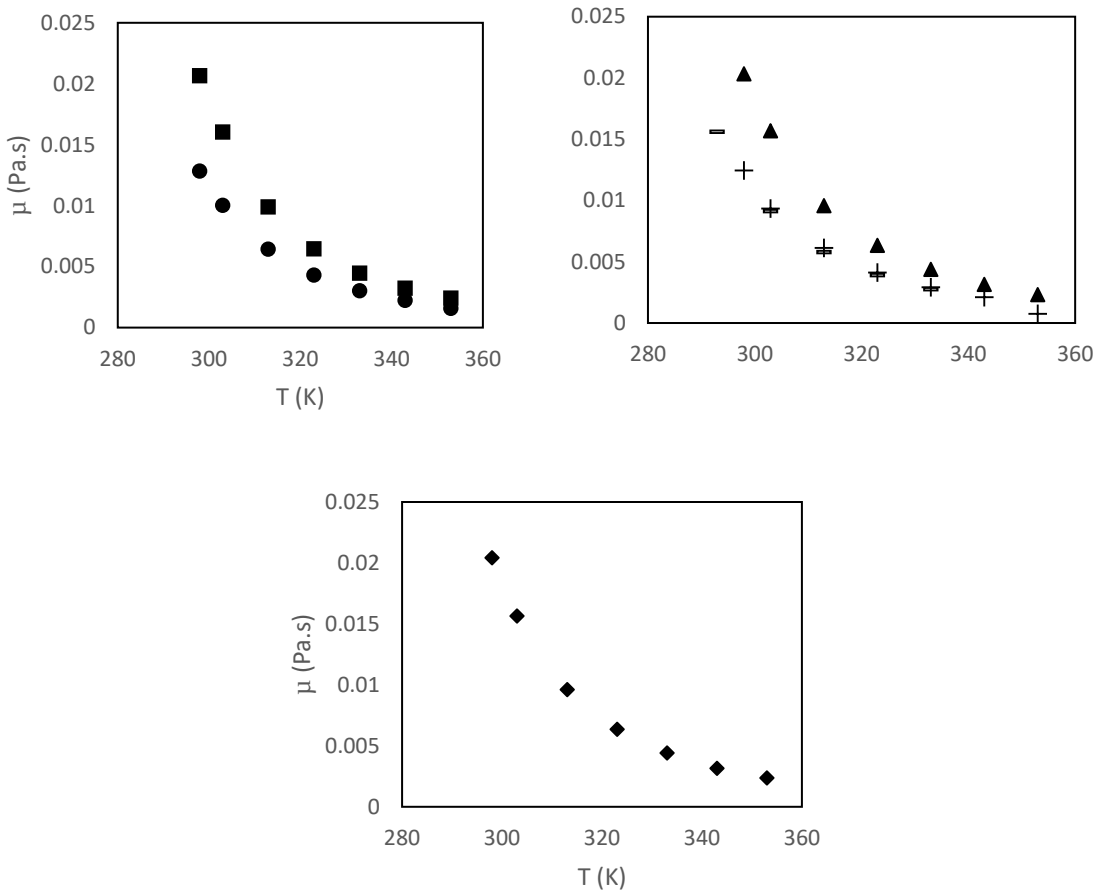

Figure 7 Dynamic viscosities (Pa.s), from 298 to 353K, of 3D2M, measured in Garcia et al. [26] (+), and in Monteiro et al. (2015) (-); 3D2M+MEG (▲),3D2M+DEG (♦); 3D2M +TEG (■) and 3D2M + CARBITOL (●).

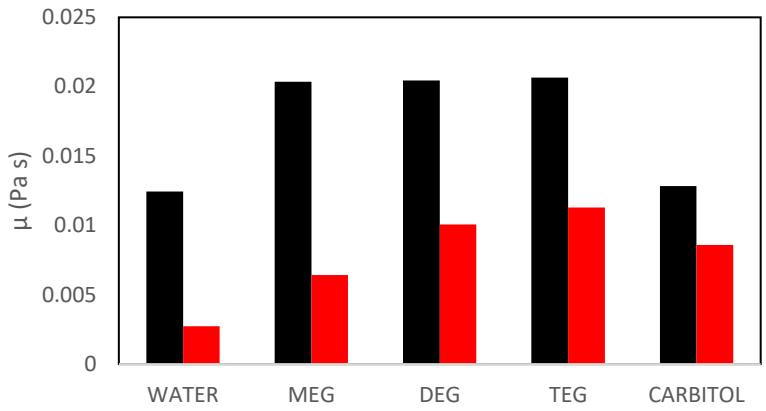

Figure 8 Dynamic viscosities (Pa.s) at 298K of 3D2M [26] 3D2M+MEG/DEG/TEG/CARBITOL/WATER (black), and 5M+MEG/DEG/TEG/CARBITOL/WATER (red)

6.3 Apparent Henry's Law Constants

The physical solubility of CO_2 has a high influence on the calculated kinetic coefficients k_{obs} and k, as seen in Equations 20 and 22. Water and 5 MEA solutions were used for the validation of the N_2O solubility equipment used in this work by means of the Henry´s law constants. As seen in Figure 5 (left), the Henry´s law constant of N_2O in water increases with temperature. Values measured in this work agree with the literature, with an AARD (Equation 13) of 4.27% (Table 7). Figure 9 (right) shows the N_2O solubility in 30wt.-% MEA, in good agreement with the literature. The average AARD (Equation 13) obtained is 2.9% (Table 7).

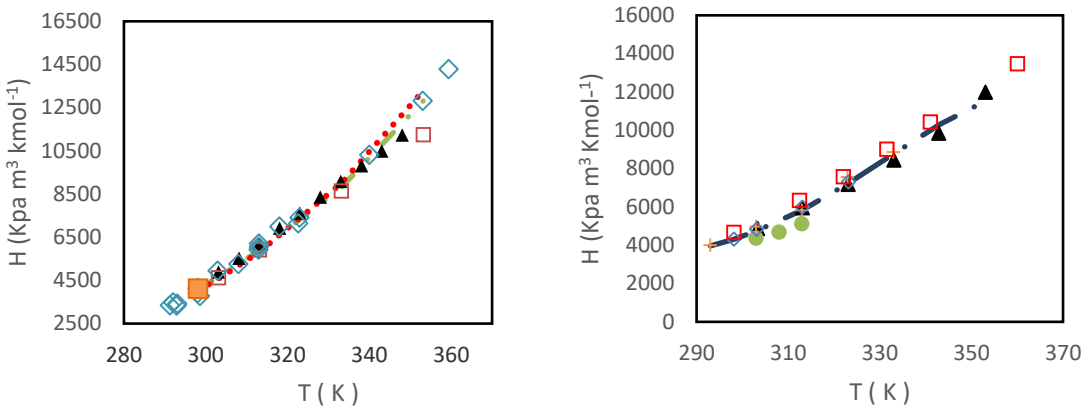

Figure 9 (Left) Apparent Henry constant of N_2O in Water (left) : this work (▲); [45](□); [42] (◊); [46] (▪) and correlation in [47] (- · -) and; (Right) Apparent Henry´s constant of N_2O in 5MEA : this work (▲), [44] (◊); [48] (●) , [49] (+);[50] (□); correlation in [47](- · -)

Table 7 AARD(%) (Equation 13) of the physical solubility of N_2O obtained in this work compared to literature

H_2O	%AARD
[46]	5.36
[42]	2.5
[47]	4.39
[50]	4.83
5MEA	%AARD
[48]	0.97
[49]	2.53
[47] (correlation)	2.91
[44]	0.98
[50] (interpolated)	7.19

Figure 10 shows the Henry´s law constants for N_2O solubility in the aqueous blends 5MEA+MEG, 5MEA+DEG, 5MEA+TEG and 5MEA+CARBITOL. The reproducibility was investigated by repeating the measurements for 5MEA+DEG and 5MEA+CARBITOL, obtaining ±3.2% and ±3.0% respectively. The averages of those repetitions are represented in Figure 10.

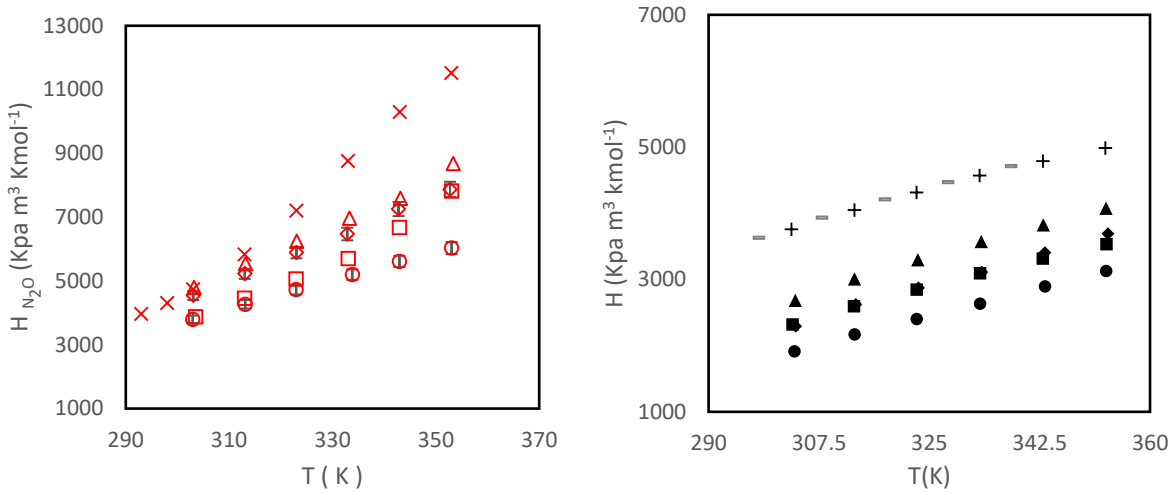

Figure 10 Henry's constants of N_2O in tested blends. 5MEA (X), 5MEA+MEG (Δ), 5MEA+DEG (◊); 5MEA+TEG (□) and 5MEA+ CARBITOL (○). Henry's constants of N_2O in aqueous solutions of 3D2M, measured in Garcia et al. [26] (+) and in Monteiro et al. [3] (-), 3D2M+MEG (▲),3D2M+DEG (♦); 3D2M +TEG (■) and 3D2M + CARBITOL (●).

As seen in Figure 10, at 303K, the lowest Henry's constants of N_2O are shown by the 5MEA+TEG and 5MEA+CARBITOL blends. At 303K, 5MEA, 5MEA+MEG and 5MEA+DEG show very similar solubility of N_2O and the addition of MEG/DEG to 5MEA solutions does not increase the physical N_2O solubility at temperatures below ~313K. The differences between the blends with added MEG, DEG, TEG and CARBITOL increase at temperatures higher than 313K, but they all show lower Henry´s law constant than that of 5MEA. Lowest values of Henry´s law constant and

thus the highest physical solubility at high temperature (343-353K) are exhibited by the 5MEA+CARBITOL blend. At 353K, the blends 5MEA+DEG/TEG show a similar N_2O solubility and 5MEA+MEG shows slightly lower N_2O solubility than those.

The results at low temperature, 298K, are different to the data from Leites [4] at 293K, where the partial pressure of CO_2 in non-aqueous blends of MEG/DEG/TEG and 2.5M MEA was measured under 13 and 104 kPa of CO_2. He reported that the highest solubility was shown by the solution containing MEG, followed by TEG and DEG (MEG>TEG>DEG). In this work, at 298K, CARBITOL showed the highest solubility of CO_2 into the solution, by meaning the lowest value of Henry´s law constant. Without considering CARBITOL, TEG would show the highest solubility of CO_2 into the solution at the lowest temperature (303K).

The physical solubility of N_2O in 3D2M+MEG/DEG/TEG/CARBITOL has the same order than that in 5MEA+MEG/DEG/TEG/CARBITOL in respect to the organic solvents (Figure 10). It means that the addition of organic solvent decreases the Henry's Law constant (increases the solubility) in the order MEG>TEG=DEG>CARBITOL. Figure 7 shows clearly that the N_2O solubility increases by the addition of organic solvents even at low temperatures. However, in blends of MEA with organic solvents the solubility was influenced only slightly by the addition of organic solvents at low temperatures (Figure 10). In Figure 11, two blends of the family 3D2M (3D2M and 3D2M+DEG) are compared with its similar blends of the family 5MEA (5MEA and 5MEA+DEG). As seen in Figure 11, the blends of the family 3D2M have higher N_2O solubility than those of 5MEA. Moreover, the influence of the temperature in the Henry's Law constant values is stronger in the case of the 5MEA blends compared to the 3D2M blends, as observed on the slope of the trend lines (Figure 11).

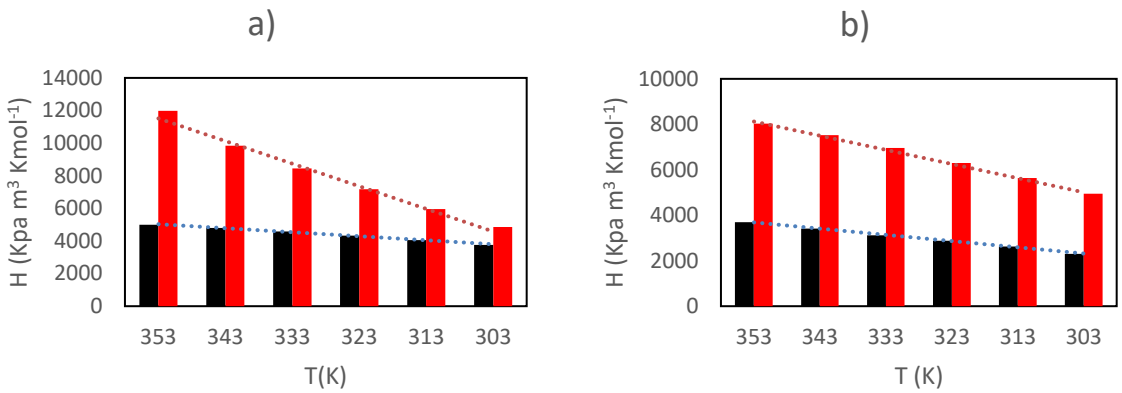

Figure 11 Comparison of N_2O Henry's Law constant in blends 3D2M and 3D2M+DEG with 5MEA and 5MEA+DEG: a)3D2M (black), MEA (red); b) 3D2M+DEG(black), 5MEA+DEG (red); Lines represent the trend line of the bars.

6.5 Vapour pressure

The vapour pressures of unloaded 5MEA, 5MEA+MEG/DEG/TEG/CARBITOL, 3D2M and 3D2M+ MEG/DEG/TEG/CARBITOL were recorded during the stirred cell experiments before CO_2 was added. The results are represented in Figure 12. As seen in this graph, the highest vapour pressure is observed in 30wt.-% MEA+70wt.-% H_2O. The vapour pressure of 5MEA+ MEG is 30 and 47% lower than that of 5MEA at 353K and 303K, respectively. 5MEA+DEG, 5MEA+TEG and 5MEA+CARBITOL exhibit vapour pressure values between 5MEA and 5MEA+MEG. The same behavior is seen for the 3D2M solutions: 3D2M+MEG shows the lowest values and 3D2M the highest, while the rest of the blends show very similar results. First it should be noted that the vapor pressure of pure MEG, DEG and TEG are 10-100 times smaller compared to the amines that has much lower vapor pressures compared to water. Pure CARBITOL has a vapor pressure which is the same order of magnitude to that of the amines. Furthermore, water is present in high

concentrations in all of the solutions (57 to 88 mol%) as shown in Table 4. Thus the vapor pressure above the solution is strongly dominated by the water vapor pressure, for example explaining minimum of 95% of the total pressure at 293K. In the blends with organic solvents, the vapor pressure over the solution decreases due to the decrease of water content in the solution , seen Table 4. Similarly, the mol% of DEG, TEG and CARBITOL is quite similar, whereas the amount of moles of MEG is higher in the solution due to the lower molar weight of MEG. Thus, the mol% of water in the MEG solutions decreases leading into the lowest vapor pressure.

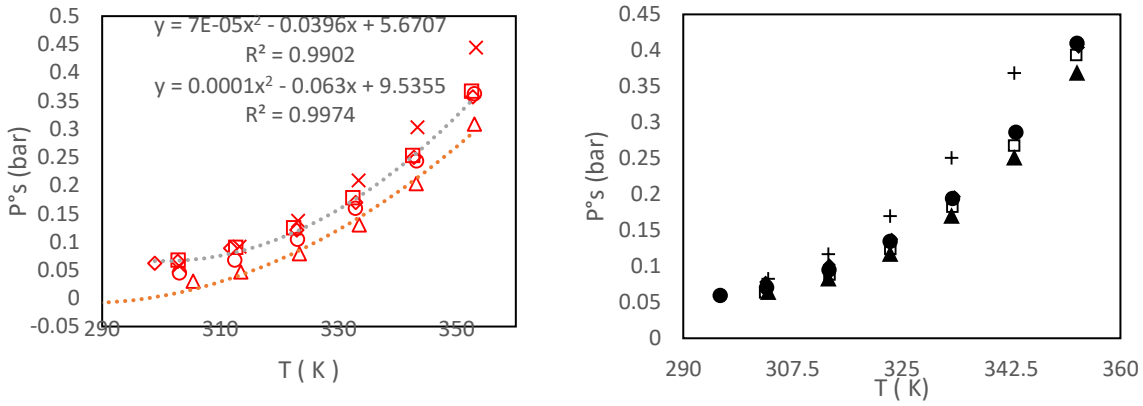

Figure 12 (Left) Vapour pressures ($P°_s$) of 5MEA (X), 5MEA+MEG (Δ), 5MEA+DEG (◊); 5MEA+TEG (□) and 5MEA+ CARBITOL (○) ; (Right) 3D2M, measured in Garcia et al. [26] (+), 3D2M+MEG (▲),3D2M+DEG (♦); 3D2M +TEG (■) and 3D2M + CARBITOL (●)

6.4 Kinetics

6.4.1 5MEA

The mass transfer coefficients k'_G measured in this work (Equation 21) and shown in Figure 13 , are in agreement with the experimental work from Luo et al.[51] and Puxty et al.[52]. At low temperatures, below 333K, the agreement is very good. The experiments were repeated at

temperatures 298, 303, 308, 313,318, 323 and 333K. As shown in the figure, the repeatability was good even though the variation seemed to be slightly higher compared to data of Luo et al.[51], who compared the results using a wetted wall column (WWC) and a string of discs contactor (SDC), through a proposed soft model, concentration-based model by direct mechanism and activity-based model by direct mechanism. No literature data has been previously reported above temperature of 343K.

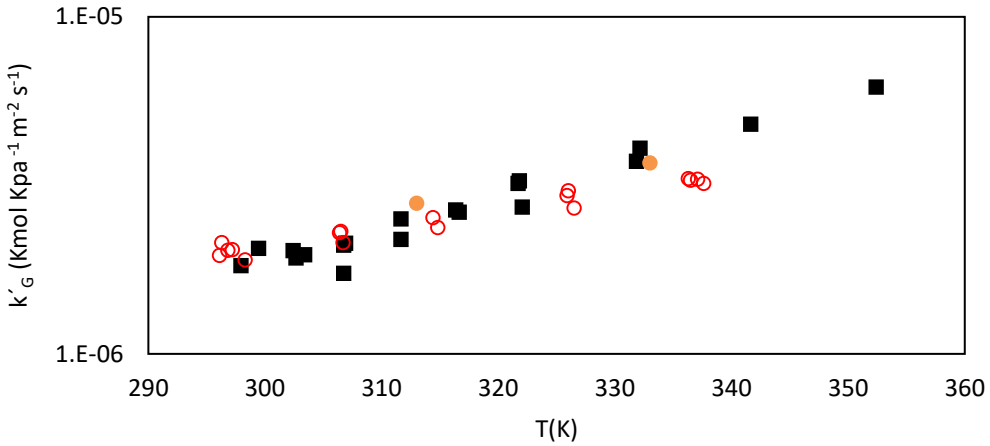

Figure 13 Measured mass transfer coefficient (K'_G) for the absorption of CO_2 into unloaded 5MEA solutions and previous values reported in literature: Experimental values from this work (▪), from [52] (●) and from [51](○); .

The second order kinetic constant, k, calculated using Equations 20-22 is shown in Figure 14. The kinetic constant follows a linear trend in the logarithmic scale and exponential grow at (Figure 14). The results are in good agreement with the values previously reported in Ying & Eimer [35] and Aboudheir et al.[7]. Furthermore, it seems that the highest value agrees also with Luo et al.[51]. As seen in Figure 13 and Figure 14, the results of k'_G are closer to the data reported in the literature than the values of k. This is due to the influence of physical properties in calculations, as viscosities

and densities. Moreover, the models and data used in the correlations of diffusivity and the Henry´s law constant are different in the different literature sources. As mentioned by Monteiro & Svendsen [53] an underestimation of 50% in the kinetic coefficient can be caused by under-estimating the Henry´s law constant of CO_2 in the solution by approximately 22%.

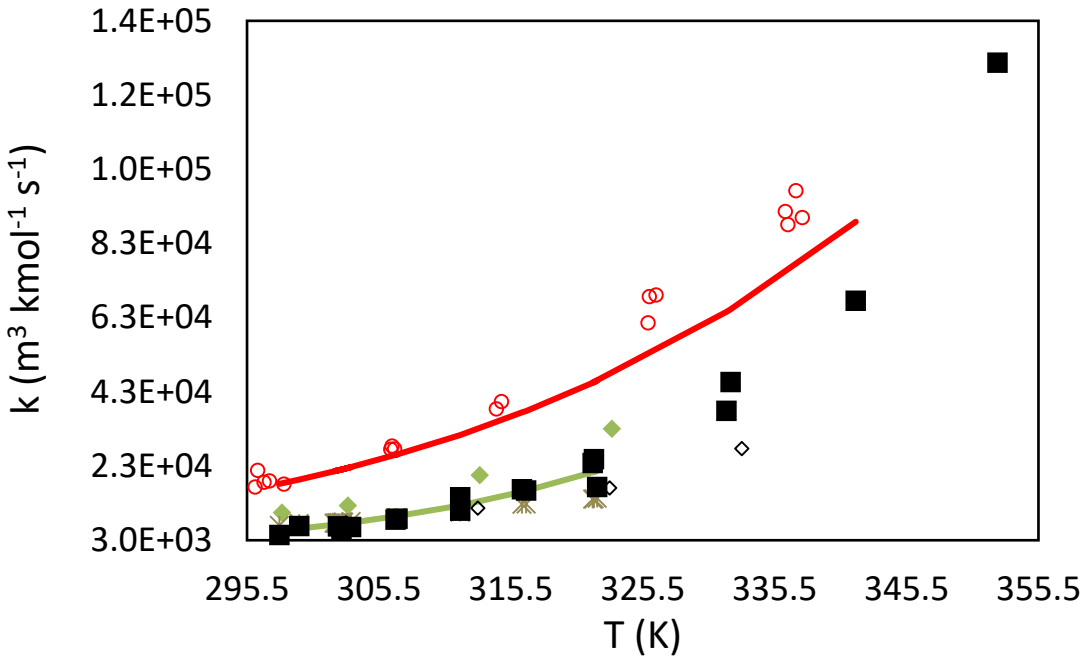

Figure 14 Measured kinetic coefficient (k) for the absorption of CO_2 into 30wt.-%MEA solutions and previous values reported in literature: Experimental values from this work (■) and from [51](○); [35] (●); [7](◊); and reinterpreted data from [7] (*); Lines represent correlations from [51] (-); and [35] (-); (*calculated from k_2 correlation by Equations 15 and 17)

6.4.2 5 MEA and 3D2M in MEG/DEG/TEG/CARBITOL + H_2O

As seen in Figure 15, the mass transfer coefficient increases as the temperature increases for all the systems. At low temperatures, 298-313K, the addition of organic solvents to 5MEA reduces

the mass transfer of CO_2 except in case of the blend 5MEA+ MEG, which maintains the same value of mass transfer coefficient as 5MEA. However, at higher temperatures (333-353K), the addition of organic solvents enhance the mass transfer of CO_2, and the use of CARBTOL and DEG show a notable increase on the mass transfer coefficients compared to those of the 5MEA solution, being 2.1 times that of 5MEA at the highest temperature. The results are in good agreement with the results of Yuan & Rochelle [10]. Although they did not use unloaded solutions, Yuan & Rochelle [10] observed an increase of the mass transfer coefficient in loaded aqueous 7m MEA solutions containing CARBITOL (in mass proportion 3:1 for water: CARBITOL) at loadings between 0.36 and 0.42 mol CO_2/mol MEA. Additionally, Yuan & Rochelle [10] observed a higher increase in solutions with higher content of CARBITOL (in mass proportion 1:3 for water: CARBITOL), in which the mass transfer increased, at loadings from 0.27 to 0.42 compared to 5MEA. However, they did not see the increase in the absorption rate for the 5MEA solution containing CARBITOL and water (3:1). In contrast to the current work where addition of DEG increased the mass transfer, Yu & Tan [12], reported that the addition of DEG to DETA+PZ solutions (in mass proportion 2:1 for water:DEG) decreased the mass transfer coefficient ($K_g a$) by 20-30%.

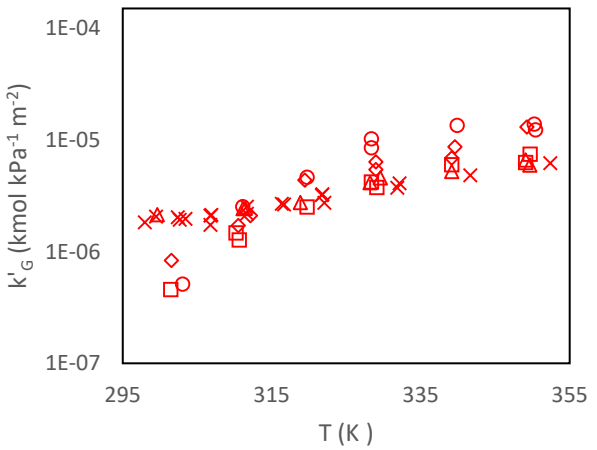

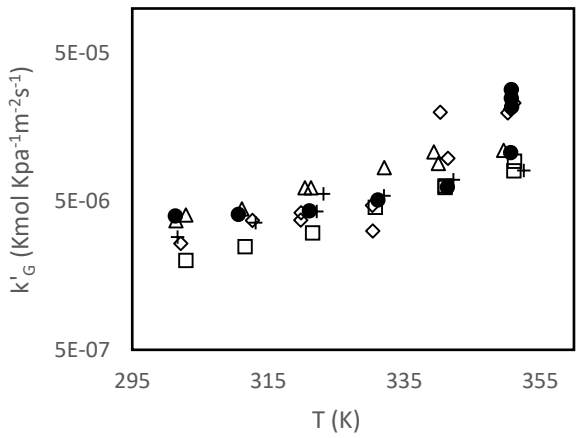

Figure 15 Mass transfer coefficient in the liquid phase k'_G. (Left) 5MEA (X), 5MEA+MEG (Δ), 5MEA+DEG (◊); 5MEA+TEG (□) and 5MEA+ CARBITOL (○); (Right) 3D2M [26] (*), 3D2M+MEG (Δ),3D2M+DEG (◊); 3D2M +TEG (□) and 3D2M + CARBITOL (●)

Below 303K, as in the case of the mass transfer coefficient k'_G, the blends containing organic solvents have lower kinetic coefficients than 5MEA with the exception of 5MEA+ MEG as shown in Figure 16. All the studied systems have higher observed kinetic coefficient than 5MEA from 313K to 353K with higher increase at the highest temperature. The blends 5MEA+DEG and 5MEA+CARBITOL show the highest kinetic coefficients, 4.6 and 3.1 times the value of that of 5MEA, respectively ($1.3 \cdot 10^6$ and $2.1 \cdot 10^6$ $m^3 kmol^{-1} s^{-1}$ increase). As seen in Figure 15 and Figure 16, the difference between the kinetic coefficients of the different blends is not as high as the difference between the mass transfer coefficients, mainly due to the influence of the physical solubility (Henry´s law constant) (Equation 20). As seen in Figure 10, the blend 5MEA+ CARBITOL shows the lowest value of Henry´s law constant while the values for 5MEA+ DEG are between the blends 5MEA+ MEG and 5MEA+TEG. However, although the higher Henry´s law constant affects the kinetic constants and consequently the difference in k_{obs} between the blends becomes smaller, the systems with the highest overall mass transfer coefficient have also the highest k_{obs} (5MEA+ CARBITOL and 5MEA+DEG).

Moreover, the diffusivity of CO_2 in the solution decreases as the viscosity of the solution increases (Equation 29). As seen from Equation 20, the kinetic coefficient k_{obs} is inversely proportional to the diffusivity. The influence of the diffusivity is not as high as that of the Henry´s law constant, as the k_{obs} is proportional to the square of the Henry´s constant. Moreover, there is a small variability of the diffusivity between the blends. While the Henry´s law constant varies in order of magnitude, the viscosity is in the same order of magnitude for all the blends studied. As seen in

Figure 6, the blends with TEG, DEG and CARBITOL (5MEA+TEG, 5MEA+DEG and 5MEA+CARBITOL) have the highest viscosities.

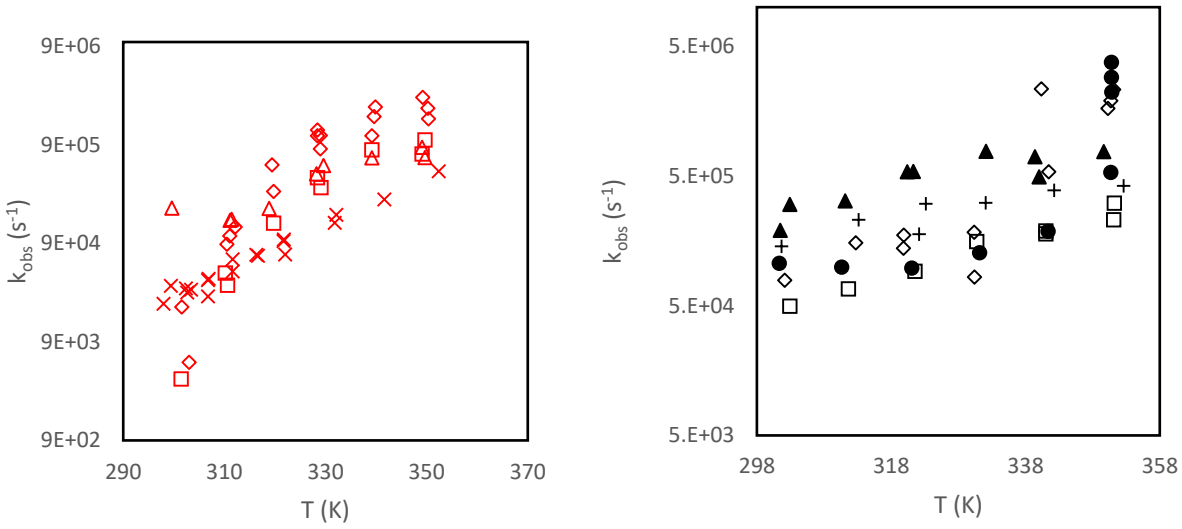

Figure 16 Observed kinetic constant, k_{obs}. (Left) 5MEA (X), 5MEA+MEG (Δ), 5MEA+DEG (◊); 5MEA+TEG (□) and 5MEA+ CARBITOL (○), (Right)3D2M, measured in Garcia et al. [26] (+), 3D2M+MEG (▲),3D2M+DEG (♦); 3D2M +TEG (■) and 3D2M + CARBITOL (●)

In case of 3D2M systems, at low temperature, 303-333K, all systems expect 3D2M+MEG show lower mass transfer coefficient k'_G compared to 3D2M. From 343 to 353K, 3D2M and 3D2M+TEG exhibited similar mass transfer coefficient. However, the addition of CARBITOL and DEG increases the k'_G to the highest values. The results at higher temperature show similar results as the 5MEA systems, and the mass transfer coefficient, k'_G, of 3D2M+CARBITOL was 2.4 times higher than that of 3D2M at 353K.

The observed kinetic coefficients from 303 to 353K of 3D2M and 3D2M+MEG/DEG/TEG/CARBITOL solutions are included in Figure 16 . From 303 to 343K, 3D2M+DEG, 3D2M+TEG and 3D2M+ CARBITOL exhibit similar kinetic coefficient than

3D2M. 3D2M+MEG, however, shows higher observed kinetic coefficient than 3D2M. Finally, Figure 15 shows that, although the mass transfer coefficients of 3D2M+CARBITOL (black circles) are higher than those of 3D2M (black crosses), the influence of the physical properties (Equations 20,22 and 29) results in lower kinetic coefficients of the absorption of CO_2 in 3D2M+CARBITOL compared to that in 3D2M, as seen in Figure 16. However, it can be seen that at high temperature, the addition of organic components increases the observed kinetic coefficient compared to 3D2M, with the exception of the blend 3D2M+ TEG. That strong difference between the influence of organic solvents at low and high temperature can be due to the existence of DEEA clusters, as suggested by Monteiro et al. [3]. Those clusters are stronger at low temperature and could enclose MAPA molecules, which are the ones reacting faster with the CO_2. The substitution of water by organic solvents, which are bigger molecules,leaves even less space between the clusters for the CO_2 molecules to react. However, at higher temperature, the DEEA clusters are weaker and the higher solubility of CO_2 into the blends containing organic solvents increase the available CO_2 which can react with free molecules of MAPA.

The results are summarized in Figure 17 and Figure 18. The figures clearly shows that:

- at low temperatures substitution of part of the water with a organic solvent doesn't have a significant difference on the mass transfer coefficients or the kinetic constant.

- At high temperatures the substitution of water with CARBITOL and DEG seems have a large influence for both amine systems.

- Both TEG and MEG show slightly higher values compared to 5MEA and 3D2M but the difference is not very large.

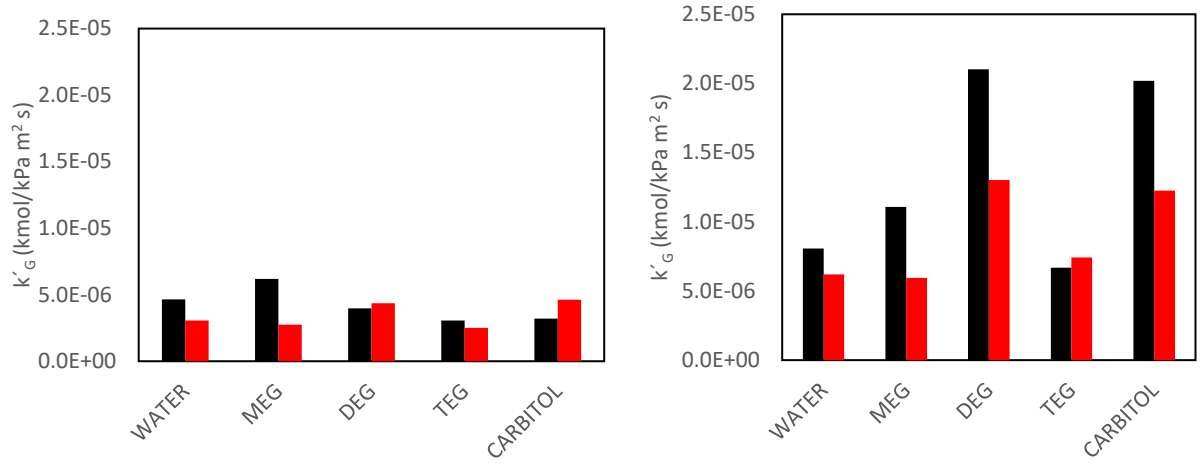

Figure 17 Mass transfer coefficient $k´_G$ (kmol Kpa^{-1} m^{-2} s^{-1}) of studied 3D2M (black) and 5MEA (red) systems at 323K (left) and 353K (right).

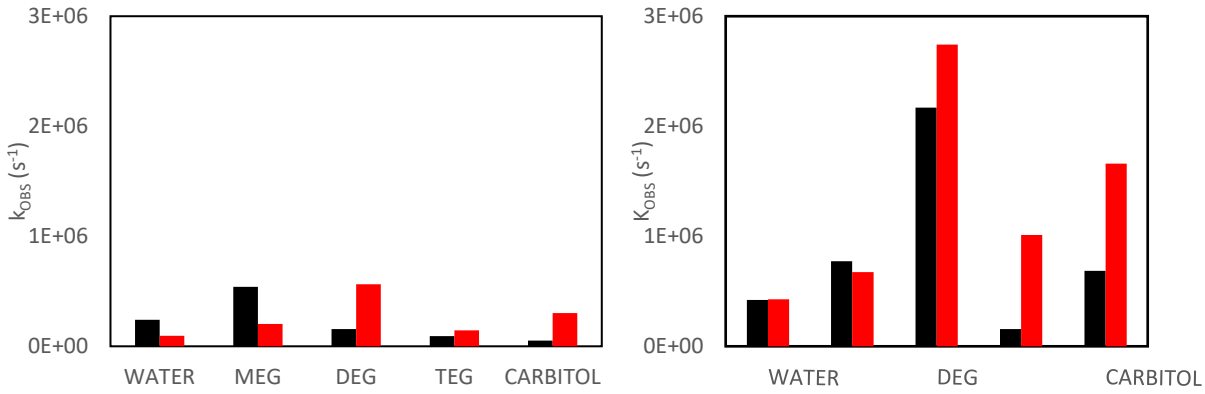

Figure 18 Observed kinetic k_{obs} (s^{-1}) of aqueous 3D2M, 3D2M+MEG/DEG/TEG/CARBITOL (black); and aqueous 5MEA, 5MEA+ MEG/DEG/TEG/CARBITOL (red), at 323 K (left) and 353 K (right)

As included in the work of Sada et al. [29], there is a relation between the second-order reaction rate constant and the dielectric constant of the dilution media. In this work, as in Sada et al [29], the dielectric constant has been studied relative to the dilution media and was estimated as the sum

of the contribution of each solvent (water and organic solvent), as included in Equation 32 [54]. To note that those values are not absolute but relative and are used for comparison of the mixtures within the two groups of amine solutions.

$$\varepsilon_m = \emptyset_1 \varepsilon_1 + \varepsilon_2 \emptyset_2 \quad (32)$$

Where ε_m is the dielectric constant of the mixture, ε_1 and ε_2 are the dielectric constants of water and the organic solvents respectively, and $\emptyset_1$ and $\emptyset_2$ are the mass fraction of water and organic solvents in the dilution media. The method was validated for the solution of water and MEG, as showed in Figure 19. The results show an acceptable results, but seem to under-predict the results from Akerlof [55], with an AARD of 6.50%.

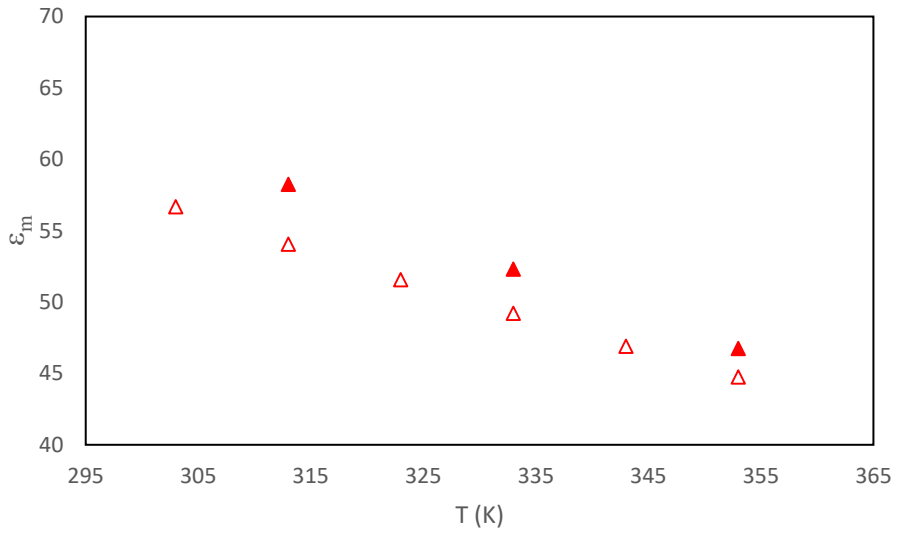

Figure 19 Dielectric constant of 50wt.-% MEG+ 50wt.-% H_2O, calculated in this work (Δ) and in Akerlof [55] (▲)

Figure 19 shows the second order rated constant as a function of dielectric constant at 303 and 353K. At 303K, the kinetic coefficient of the absorption of CO_2 increases as the dielectric constant

increases, in the cases of the amine solutions containing MEG and DEG. This behaviour is as expected, based on the results of Sada et al. [29], who measured the kinetic coefficients at 303K of various non-aqueous amine systems. However, the solutions containing CARBITOL/ TEG do not follow this trend but the kinetic coefficients remain practically constant with respect to the dielectric constants in both amine systems (MEA and 3D2M). At 353K, however, there is no pattern and at high temperatures dielectric constant does not seem to explain the behaviour of kinetic coefficients at least not in systems containing water. Further studies should be done where the changes in dielectric constant is expanded and studied in a more systematic manner.

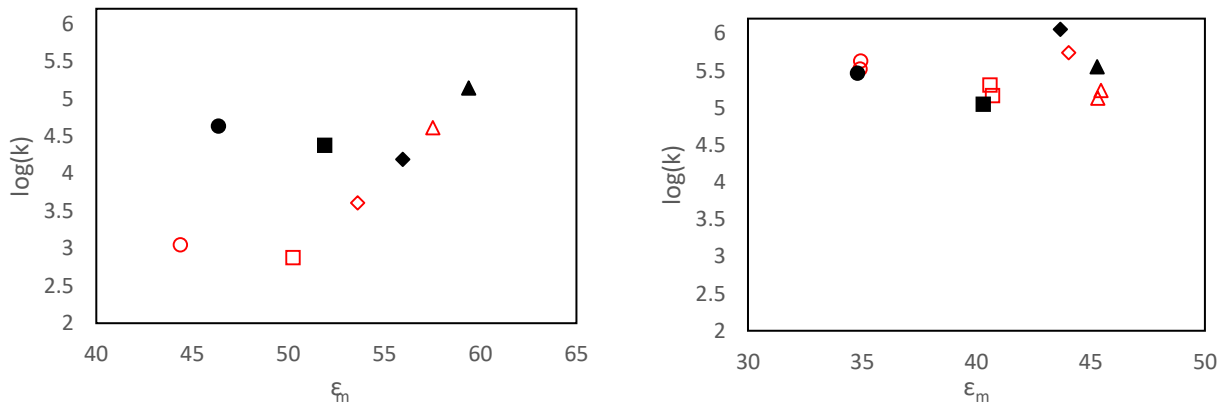

Figure 20 Logarithmic relation of the second-order reaction rate constant k of the absorption of CO_2 in the solutions and the dielectric constant of the dilution media: 5MEA+MEG (Δ), 5MEA+DEG (◊); 5MEA+TEG (□) and 5MEA+ CARBITOL (○).3D2M+MEG (▲),3D2M+DEG (♦); 3D2M +TEG (■) and 3D2M + CARBITOL (●).: (Left) approximately at 303K; (Right) approximately at 353K.

8. CONCLUSIONS

The substitution of water in aqueous amine solutions, 30 wt.-%MEA (5M MEA) solutions and 3M DEEA+ 3M MAPA (38.26wt.-% DEEA + 19.14wt.-% 3 MAPA), by organic solvents (MEG,

DEG, TEG and CARBITOL) was studied experimentally. The densities, viscosities and physical solubility of N_2O were measured from 298 to 353 K. The mass transfer coefficient, k'_G, was measured from 303 to 353K with a Double Stirred Cell (DSC).

The results show that the substitution of water by organic solvents improves the physical solubility of CO_2 and decreases the vapour pressure of the solution. However, the densities and viscosities increases. The mass transfer coefficient, k'_G, and the observed kinetic coefficient, k_{obs} increase with the addition of DEG and CARBITOL at high temperatures. At low temperatures the substitution of part of the water with organic solvent does seem to have an influence on the absorption kinetics. At higher temperature, however, from 313 to 353K, the addition of organic solvents increase the observed kinetic coefficients of the absorption of CO_2 in 5M MEA and 3D2M solutions. It will be of interest to further investigate the effect/correlation between dielectric constants and kinetic coefficients.

9. ACKNOWLEDGMENTS

This work was supported by

- the EPSRC grant EP/J020184/1 and the UK CCS Research Centre (www.ukccsrc.ac.uk). The UKCCSRC is funded by the EPSRC as part of the RCUK Energy Programme.)'
- the Access to Research Infrastructures activity in the Horizon 2020 Programme of the ET (ECCSEL INFRADEV-3 Grant Agreement n. 654028)
- The Research Council of Norway through project 3GMC (3rd Generation Solvent Membrane Contactor, Project No. 239789)

REFERENCES

[1] I. Kim, H.F. Svendsen, E. Børresen, Ebulliometric Determination of Vapor - Liquid Equilibria for Pure Water , Monoethanolamine , N -Methyldiethanolamine , 3- (Methylamino) -propylamine , and Their Binary and Ternary Solutions, (2008) 2521–2531.

[2] J.G.M.-S. Monteiro, Contributions to kinetics and equilibrium of CO2 absorption into N,N,-diethylethanolamine (DEEA), N-Methyl-1,3-propane-diamine (MAPA) and their blends, Norwegian University of Science and Technology. Faculty of Natural Sciences and Technology, 2014.

[3] J.G.M.-S. Monteiro, H. Majeed, H. Knuutila, H.F. Svendsen, Kinetics of CO2 absorption in aqueous blends of N,N-diethylethanolamine (DEEA) and N-methyl-1,3-propane-diamine (MAPA), Chem. Eng. Sci. 129 (2015) 145–155. doi:10.1016/j.ces.2015.02.001.

[4] I.. L. Leites, THERMODYNAMICS OF CO2 SOLUBILITY IN MIXTURES MONOETHANOLAMINE WITH ORGANIC SOLVENTS AND WATER AND COMMERCIAL EXPERIENCE OF ENERGY SAVING GAS PURIFICATION TECHNOLOGY, Energy Convers. Manag. 39 (1998).

[5] X. Luo, A. Hartono, H.F. Svendsen, Comparative kinetics of carbon dioxide absorption in unloaded aqueous monoethanolamine solutions using wetted wall and string of discs columns, Chem. Eng. Sci. 82 (2012) 31–43. doi:10.1016/j.ces.2012.07.001.

[6] K.R. Putta, D.D.D. Pinto, H.F. Svendsen, H.K. Knuutila, CO2 absorption into loaded aqueous MEA solutions: Kinetics assessment using penetration theory, Int. J. Greenh. Gas Control. 53 (2016) 338–353. doi:10.1016/j.ijggc.2016.08.009.

[7] A. Aboudheir, P. Tontiwachwuthikul, A. Chakma, R. Idem, Kinetics of the reactive

absorption of carbon dioxide in high CO2-loaded, concentrated aqueous monoethanolamine solutions, Chem. Eng. Sci. 58 (2003) 5195–5210. doi:10.1016/j.ces.2003.08.014.

[8] J. Tan, H. Shao, J. Xu, L. Du, G. Luo, Mixture Absorption System of Monoethanolamine Triethylene Glycol for CO2 Capture, Ind. Eng. Chem. Res. 50 (2011) 3966–3976. doi:10.1021/ie101810a.

[9] J. Song, S. Park, J. Yoon, H. Lee, S. Korea, K. Lee, Solubility of Carbon Dioxide in Monoethanolamine + Ethylene Glycol + Water and Monoethanolamine + Poly (ethylene glycol) + Water at 333 . 2 K, Engineering. 9568 (1997) 143–144.

[10] Y. Yuan, G. Rochelle, CO2 absorption rate in amine in organic / water solvent, in: Third Univ. Texas Conf. Carbon Capture Storage (UTCCS-3), Austin, Texas, USA, 2016.

[11] Y. Jiru, D.A. Eimer, A Study of Mass Transfer Kinetics of Carbon Dioxide in (Monoethanolamine + Water) by Stirred Cell, Energy Procedia. 37 (2013) 2180–2187. doi:10.1016/j.egypro.2013.06.097.

[12] C.-H. Yu, C.-S. Tan, CO 2 Capture by Aqueous Solution Containing Mixed Alkanolamines and Diethylene Glycol in a Rotating Packed Bed, Energy Procedia. 63 (2014) 758–764. doi:10.1016/j.egypro.2014.11.084.

[13] B.B. Woertz, Experiments with Solvent-Amine-Water for Removing CO2 from Gas, Can. J. Chem. Eng. 50 (1972) 425–427.

[14] A. Henni, A.E. Mather, Solubility of Carbon Dioxide in Methyldiethanolamine + Methanol + Water, J. Chem. Eng. Data. (1995) 493–495.

[15] H. Kierzkowska-Pawlak, R. Zarzycki, Solubility of carbon dioxide and nitrous oxide in

water + methyldiethanolamine and ethanol + methyldiethanolamine solutions, J. Chem. Eng. Data. 47 (2002) 1506–1509. doi:10.1021/je020093v.

[16] M.H. Oyevaar, H.J. Fonteln, K.R. Westerterp, Equilibria of carbon dioxide in solutions of diethanolamine in aqueous ethylene glycol at 298 K, J. Chem. Eng. Data. 34 (1989) 405–408. http://pubs.acs.org/doi/abs/10.1021/je00058a010.

[17] F.C. Riesenfeld, H.D. Frazier, Patent: Separation of Acidic Constituents from gases, 1952.

[18] O. Aschenbrenner, P. Styring, Comparative study of solvent properties for carbon dioxide absorption, (2010) 1106–1113. doi:10.1039/c002915g.

[19] F.-Y. Jou, F.D. Otto, A.E. Mather, Solubility of H2S and CO2 in diethylene glycol at elevated pressures, 175 (2000) 53–61.

[20] J.E. Crooks, J.P. Donnellan, Kinetics and mechanism of the reaction between carbon dioxide and amines in aqueous solution, J. Chem. Soc. Perkin Trans. 2. 2 (1989) 331. doi:10.1039/p29890000331.

[21] M. Caplow, Kinetics of carbamate formation and breakdown, J. Am. Chem. Soc. 90 (1968) 6795–6803. doi:10.1021/ja01026a041.

[22] P.B. Konduru, P.D. Vaidya, E.Y. Kenig, Activated DEEA Process for CO2 Capture, Proc. 2nd Annu. Gas Process. Symp. (2010) 21–29. doi:10.1016/S1876-0147(10)02003-3.

[23] J.G.M.-S. Monteiro, H. Knuutila, N.J.M.C. Penders-van Elk, G. Versteeg, H.F. Svendsen, Kinetics of CO2 absorption by aqueous N,N-diethylethanolamine solutions: Literature review, experimental results and modelling, Chem. Eng. Sci. 127 (2015) 1–12. doi:10.1016/j.ces.2014.12.061.

[24] J.G.M.-S. Monteiro, D.D.D. Pinto, S.A.H. Zaidy, A. Hartono, H.F. Svendsen, VLE data and modelling of aqueous N,N-diethylethanolamine (DEEA) solutions, Int. J. Greenh. Gas Control. 19 (2013) 432–440. doi:10.1016/j.ijggc.2013.10.001.

[25] M. Garcia, H.K. Knuutila, S. Gu, Thermodynamic modelling of unloaded and loaded N,N-diethylethanolamine solutions, Green Energy Environ. 1 (2016) 246–257.

[26] M. Garcia, H.K. Knuutila, S. Gu, Determination of kinetics of CO2 absorption in unloaded and loaded DEEA + MAPA blend, Energy Procedia. 114 (2017) 1772–1784.

[27] P. V. Danckwerts, The absorption of gases in liquids, Pure Appl. Chem. 10 (1965) 625–642. doi:10.1351/pac196510040625.

[28] J.G.M. Monteiro, S. Hussain, H. Majeed, E.O. Mba, A. Hartono, H. Knuutila, H.F. Svendsen, Kinetics of CO 2 Absorption by Aqueous 3- (Methylamino) propylamine Solutions : Experimental Results and Modeling, AIChE J. 60 (2014) 3792–3803. doi:10.1002/aic.

[29] E. Sada, H. Kumazawa, Z.Q. Han, Kinetics of Reaction Between Carbon Dioxide and Ethylenediamine in Non- aqueous Solvents, Chem. 31 (1985) 109–115.

[30] U.E. Aronu, A. Hartono, H.F. Svendsen, Density, viscosity, and N2O solubility of aqueous amino acid salt and amine amino acid salt solutions, J. Chem. Thermodyn. 45 (2012) 90–99. doi:10.1016/j.jct.2011.09.012.

[31] D.D.D. Pinto, J.G.M.-S. Monteiro, B. Johnsen, H.F. Svendsen, H. Knuutila, Density measurements and modelling of loaded and unloaded aqueous solutions of MDEA (N-methyldiethanolamine), DMEA (N,N-dimethylethanolamine), DEEA

(diethylethanolamine) and MAPA (N-methyl-1,3-diaminopropane), Int. J. Greenh. Gas Control. 25 (2014) 173–185. doi:10.1016/j.ijggc.2014.04.017.

[32] S. Gondal, N. Asif, H.F. Svendsen, H. Knuutila, Density and N2O solubility of aqueous hydroxide and carbonate solutions in the temperature range from 25 to 80ºC, Chem. Eng. Sci. 122 (2015) 307–320. doi:10.1016/j.ces.2014.09.016.

[33] E. Sada, H. Kumazawa, M.A. Butt, Solubilities of Gases in Aqueous Solutions of Amine, Engineering. 22 (1977) 1975–1976. doi:10.1021/je60074a011.

[34] R.J. Littel, G.F. Versteeg, W.P.M. Van Swaaij, Kinetics of CO2 with primary and secondary amines in aqueous solutions—I. Zwitterion deprotonation kinetics for DEA and DIPA in aqueous blends of alkanolamines, Chem. Eng. Sci. 47 (1992) 2027–2035. doi:10.1016/0009-2509(92)80319-8.

[35] J. Ying, D. a. Eimer, Determination and measurements of mass transfer kinetics of CO2 in concentrated aqueous monoethanolamine solutions by a stirred cell, Ind. Eng. Chem. Res. 52 (2013) 2548–2559. doi:10.1021/ie303450u.

[36] W. Khan, An extension of Danckwerts theoretical surface renewal model to mass transfer at contaminated turbulent interfaces, Math. Comput. Model. 14 (1990) 750–754. doi:10.1016/0895-7177(90)90282-R.

[37] A. Jamal, Absorption and Desorption of CO2 and CO in Alkanolamine Systems, The University of British Columbia, 2002.

[38] L. Kucka, J. Richter, E.Y. Kenig, a. Górak, Determination of gas-liquid reaction kinetics with a stirred cell reactor, Sep. Purif. Technol. 31 (2003) 163–175. doi:10.1016/S1383-

5866(02)00179-X.

[39] H. Hikita, Haruo, Ishikawa, Physical absorption in Agitated Vessels with a Flat Gas-Liquid Interface, J. Chem. Inf. Model. 53 (1969) 160. doi:10.1017/CBO9781107415324.004.

[40] R.J. Littel, G.F. Versteeg, W.P.M. Van Swaaij, Physical absorption into non-aqueous solutions in a stirred cell reactor, Chem. Eng. Sci. 46 (1991) 3308–3313. doi:10.1016/0009-2509(91)85036-W.

[41] L. Korson, W. Drost-Hansen, F.J. Millero, Viscosity of water at various temperatures, J. Phys. Chem. 73 (1969) 34–39. doi:10.1021/j100721a006.

[42] G.F. Versteeg, W.P.M. Van Swaaij, Solubility and diffusivity of acid gases (carbon dioxide, nitrous oxide) in aqueous alkanolamine solutions., J. Chem. Eng. Data. 33 (1988) 29–34. doi:10.1021/je00051a011.

[43] D. a. Glasscock, J.E. Critchfield, G.T. Rochelle, CO2 absorption/desorption in mixtures of methyldiethanolamine with monoethanolamine or diethanolamine, Chem. Eng. Sci. 46 (1991) 2829–2845. doi:10.1016/0009-2509(91)85152-N.

[44] J. Ying, D.A. Eimer, Measurements and Correlations of Diffusivities of Nitrous Oxide and Carbon Dioxide in Monoethanolamine + Water by Laminar Liquid Jet, Ind. \& Eng. Chem. Res. 51 (2012) 16517–16524. doi:10.1021/ie302745d.

[45] F.-Y. Jou, A.E. Mather, F.D. Otto, The solubility of CO2 in a 30 Mass Percent Monoethanolamine Solution, Can. J. Chem. Eng. 73 (1995) 140–147.

[46] A.K. Saha, S.S. Bandyopadhyay ', A.K. Biswas, Solubility and Diffusivity of N20 and C02 in Aqueous Solutions of 2-Amino-2-methyl-1 -propanol, J. Chem. Eng. Data. 38 (1993) 78–

82. doi:10.1016/S0261-3069(96)90061-8.

[47] S. Ma'mun, H.F. Svendsen, Solubility of N2O in aqueous monoethanolamine and 2-(2-Aminoethyl-amino)ethanol solutions from 298 to 343 K, Energy Procedia. 1 (2009) 837–843. doi:10.1016/j.egypro.2009.01.111.

[48] L. Meng-Hui, Ming-Der, Solubility and Diffusivity of N2O and Co2 in (Monoethanolamine+ N-Methyldiethanolamine+ Water) and in (Monoethanolamine + 2-Amino-2-methyl-1-propanol + Water), J. Chem. Inf. Model. 40 (1995) 486–492. doi:10.1017/CBO9781107415324.004.

[49] B. Yaghi, O. Houache, Solubility of nitrous oxide in alkanolamine aqueous solutions, J. Eng. Comput. Archit. 2 (2008). doi:10.1021/je990253b.

[50] A. Hartono, E.O. Mba, H.F. Svendsen, Physical Properties of Partially CO 2 Loaded Aqueous Monoethanolamine (MEA), J. Chem. Eng. Data. 59 (2014) 1808–1816.

[51] X. Luo, A. Hartono, S. Hussain, H. F. Svendsen, Mass transfer and kinetics of carbon dioxide absorption into loaded aqueous monoethanolamine solutions, Chem. Eng. Sci. 123 (2015) 57–69. doi:10.1016/j.ces.2014.10.013.

[52] G. Puxty, R. Rowland, M. Attalla, Comparison of the rate of CO2 absorption into aqueous ammonia and monoethanolamine, Chem. Eng. Sci. 65 (2010) 915–922. doi:10.1016/j.ces.2009.09.042.

[53] J.G.M. Monteiro, H.F. Svendsen, The N2O analogy in the CO2 capture context : Literature review and thermodynamic modelling considerations, Chem. Eng. Sci. 126 (2015) 455–470. doi:10.1016/j.ces.2014.12.026.

[54] S. Prakongpan, T. Nagai, Solubility of Acetaminophen in Cosolvents, Chem. Pharm. Bull. 32 (1984) 340–343.

[55] G. Akerlof, Dielectric Constants of Some Organic Solvent-Water Mixtures At Various Temperatures, J. Am. Chem. Soc. 54 (1932) 4125–4139. doi:10.1021/ja01350a001.

APPENDIX

Table A1 Densities (g/cm^3) of 30wt.-%MEA+35wt.-%H_2O+35wt.-%H_2O/MEG/DEG/TEG/CARBITOL

T(ºC)	H_2O	MEG	DEG	TEG	CARBITOL
25	1.010	1.054	1.059	1.062	1.023
30	1.008	1.051	1.056	1.058	1.020
40	1.003	1.044	1.049	1.051	1.012
50	0.998	1.037	1.043	1.044	1.004
60	0.992	1.030	1.035	1.036	0.995
70	0.986	1.023	1.028	1.029	0.987
80	0.979	1.015	1.021	1.021	0.978

Table A2 Densities (g/cm^3) of 39.3wt.-% DEEA- 19.1wt.-%MAPA-21.3wt.-%H_2O+21.3wt.-% MEG/DEG/TEG/CARBITOL

T (ºC)	3D2M+MEG	3D2M+DEG	3D2M+TEG	3D2M+CARBITOL
25	0.970	0.973	0.973	0.949
25	0.970	0.973	0.973	0.949
30	0.965	0.969	0.969	0.945
30	0.965	0.969	0.969	0.9445
40	0.957	0.960	0.960	0.935
40	0.957	0.959	0.960	0.935
50	0.948	0.951	0.951	0.926
50		0.951	0.951	0.926
60	0.940	0.943	0.943	0.919
60	0.940	0.943	0.942	0.919
70	0.930	0.931	0.931	0.905

70	0.931	0.932	0.931	0.905
80	0.921	0.915	0.917	0.889
80	0.921	0.912		

Table A3 Measured viscosities of 30wt.-%MEA+35wt.-%H_2O+35wt.-%H_2O/MEG/DEG/TEG/CARBITOL

T (ºC)	MEA+WATER	MEA+MEG	MEA+TEG	MEA+CARBITOL	MEA+DEG
25	0.0027	0.0074	0.0113	0.0086	0.0101
30	0.00221	0.0064	0.0091	0.0072	0.0084
40	0.00177	0.0047	0.0063	0.0050	0.0060
50	0.00137	0.0036	0.0047	0.0036	0.0041
60	0.00123	0.0029	0.0036	0.0027	0.0033
70	0.00102	0.0022	0.0030	0.0023	0.0025
80	0.00085	0.0019	0.0025	0.0018	0.00219

Table A4 Measured viscosities of 39.3wt.-% DEEA- 19.1wt.-%MAPA-21.3wt.-%H_2O+21.3wt.-% MEG/DEG/TEG/CARBITOL

T (ºC)	3D2M+MEG	3D2M+DEG	3D2M+TEG	3D2M+CARBITOL
25	0.020345	0.020438	0.020663	0.012843
30	0.015676	0.01566	0.016042	0.010038
40	0.0095888	0.0096143	0.00990571	0.0064273
50	0.0063275	0.0063621	0.006455	0.0043152
50	0.004372	0.0044223	0.0044673	0.0030202
70	0.0031419	0.0031537	0.0032277	0.0022312
80	0.0023222	0.002366	0.0024122	0.0015613

Table A5 Henry´s Law Constant of N_2O in 30wt.-%MEA+ 35wt.-% H_2O+ 35wt.-% H_2O/MEG/DEG/TEG/CARBITOL

MEA+H_2O		MEA+DEG		MEA+DEG		MEA+MEG		MEA+TEG		MEA+ CARBITOL	
T (ºC)	H (Kpa m^3 Kmol$^{-1)}$	T (ºC)	H (Kpa m^3 Kmol^{-1})	T (ºC)	H (Kpa m^3 Kmol^{-1})	T (ºC)	H (Kpa m^3 Kmol^{-1})	T (ºC)	H (Kpa m^3 Kmol^{-1})	T (ºC)	H (Kpa m^3 Kmol^{-1})
80.1	11985	79.8	7869	79.4	8035	80.3	8682	80.0	7816	79.8	6085
69.9	9851	69.8	7253	69.9	7525	70.1	7584	69.9	6671	70.5	5732
60.1	8446	59.9	6472	59.9	6961	60.3	6961	60.1	5701	60.1	5335
50.1	7176	50.0	5890	50.0	6293	50.1	6235	49.9	5053	50.2	4901
40.1	5962	40.0	5224	39.9	5633	40.1	5543	40.0	4450	40.2	4453
30.3	4863	30.1	4541	29.8	4943	30.2	4792	30.5	3875	30.5	3990

Table **A6** Henry´s Law Constant of N2O in 39.3wt.-% DEEA- 19.1wt.-%MAPA-21.3wt.-%H_2O+21.3wt.-% MEG/DEG/TEG/CARBITOL

3D2M+MEG		3D2M+DEG		3D2M+TEG		3D2M+CARBITOL	
T (ºC)	H (Kpa m^3 Kmol^{-1})	T (ºC)	H (Kpa m^3 Kmol^{-1})	T (ºC)	H (Kpa m^3 Kmol^{-1})	T (ºC)	H (Kpa m^3 Kmol^{-1})
80	4067	80.3	3692	80.1	3532	80.1	3124
70.1	3820	70.3	3408	70	3316	70.4	2896
60.2	3565	60.3	3111	60.1	3091	60.1	2635

50.2	3291	50.3	2874	50	2846	50	2399
40.2	2998	40.4	2621	40.1	2593	40.2	2169
30.7	2676	30.8	2296	30.3	2320	30.6	1913

Table A7 Mass transfer and observed kinetic constant of the absorption of CO_2 in 30wt.-%MEA+ 70wt.-% H_2O

T (ºC)	K'_G (kmol kPa^{-1} m^{-2} s)	K_{obs} (s^{-1})
24.8	1.8E-06	27308
26.3	2.1 E-06	35441
29.25	2.0 E-06	35858
30.25	2.0 E-06	34365
29.5	2.0 E-06	32548
33.75	2.1 E-06	42208
33.6	1.7 E-06	27927
33.6	2.1 E-06	41032
38.5	2.2 E-06	47519
38.5	2.5 E-06	62958
43.2	2.7 E-06	75577
43.5	2.6 E-06	73736
48.65	3.3 E-06	120644
48.9	2.7 E-06	84289
48.55	3.2 E-06	116358
58.7	3.7 E-06	176516
59	4.1 E-06	212236
68.5	4.8 E-06	324843

79.25	6.2 E-06	598871

Table A8 Mass transfer and observed kinetic constant of the absorption of CO_2 in unloaded 30wt.-%MEA + 35wt.-% H_2O + 35.-% MEG

T (ºC)	K'_G (kmol kPa^{-1} m^{-2} s)	K_{obs} (s^{-1})
26.5	2.1 E-06	204819
38.3	2.4 E-06	157946
38	2.4 E-06	154704
45.7	2.7 E-06	203621
56.45	4.6 E-06	557287
55.05	4.1 E-06	459377
66	5.2 E-06	663131
75.95	6.6 E-06	849952
76.5	5.9 E-06	673003

Table A9 Mass transfer and observed kinetic constant of the absorption of CO_2 in unloaded 30wt.-%MEA + 35wt.-% H_2O + 35.-% DEG

T (ºC)	K'_G (kmol kPa^{-1} m^{-2} s)	K_{obs} (s^{-1})
28.4	8.3E-07	20317
37.35	1.7E-06	87997
39	2.1E-06	132459
46.3	4.4E-06	563465
55.85	6.4E-06	1124498
55.85	5.4E-06	820082
66.45	8.7E-06	1747108
66	6.9E-06	1115603
76.1	1.3 E05	2743327

Table A10 Mass transfer and observed kinetic constant of the absorption of CO_2 in unloaded 30wt.-%MEA + 35wt.-% H_2O + 35.-% TEG

T (ºC)	K'_G (kmol kPa^{-1} m^{-2} s)	K_{obs} (s^{-1})
28.3	4.6E-07	3784
37.5	1.3 -06	33963
37.05	1.5E-06	44925
46.6	2.5E-06	144488
52.25	4.2E-06	417100
55.95	3.5E-06	330911
66	6.0E-06	800885
75.95	6.3E-06	729916
76.55	7.4E-06	1011813

Table A11 Mass transfer and observed kinetic constant of the absorption of CO_2 in unloaded 30wt.-%MEA + 35wt.-% H_2O + 35.-% CARBITOL

T (ºC)	k'_G (kmol kPa^{-1} m^{-2} s)	k_{obs} (s^{-1})

29.9	5.1E-07	5566
37.9	2.5E-06	107107
46.6	4.6E-06	302971
55.2	8.5E-06	877571
55.2	1.0E-05	1276356
66.7	1.4E-05	2184871
77.1	1.4E-05	2116546
77.2	1.2E-05	1659289

Table A12 Mass transfer and observed kinetic constant of the absorption of CO_2 in unloaded 39.3wt.-% DEEA- 19.1wt.-%MAPA-21.3wt.-%H_2O+21.3wt.-% MEG

T (ºC)	k'_G (kmol/kPa m^2 s)	k_{obs} (s^{-1})
29.9	4.1E-06	302418
28.45	3.7E-06	190872
38.15	4.5E-06	321117
48.3	6.2E-06	543238
47.4	6.2E-06	538425
59.1	8.5E-06	774347
66.4	1.1E-05	703645
67.05	9.0E-06	492450
76.65	1.1E-05	773801

Table A13 Mass transfer and observed kinetic constant of the absorption of CO_2 in unloaded 39.3wt.-% DEEA- 19.1wt.-%MAPA-21.3wt.-%H_2O+21.3wt.-% DEG

T (ºC)	k'_G (kmol/kPa m^2 s)	k_{obs} (s^{-1})
29.1	1.7E-06	32794
39.7	3.7E-06	148147
46.8	4.2E-06	176190
46.8	3.7E-06	139863
57.3	4.7E-06	189986
67.3	1.2E-05	2568479
68.4	9.7E-06	582426
77.2	2.0E-05	1903053
78.1	2.3E-05	2628367
77.7	2.1E-05	2168296

Table A14 Mass transfer and observed kinetic constant of the absorption of CO_2 in unloaded 39.3wt.-% DEEA- 19.1wt.-%MAPA-21.3wt.-%H_2O+21.3wt.-% TEG

T (ºC)	k'_G (kmol/kPa m^2 s)	k_{obs} (s^{-1})
30	2E-06	49675
39	2.5E-06	67572
48.5	3.1E-06	92069
57.7	4.6E-06	156263
68.1	6.2E-06	179417
78.1	8.1E-06	230001
78.2	9.3E-06	309327
77.8	6.7E-06	157840

Table A15 Mass transfer and observed kinetic constant of the absorption of CO_2 in unloaded 39.3wt.-% DEEA- 19.1wt.-%MAPA-21.3wt.-%H_2O+21.3wt.-% CARBITOL

T (ºC)	k'_G (kmol/kPa m^2 s)	k_{obs} (s^{-1})
28.3	4.1E-06	90133
38.6	3.2E-06	50880
37.6	4.6E-06	93260
58.1	4.8E-06	74905
57.5	6.0E-06	117733
68.4	4.1E-06	54771
77.8	1.8E-05	535004
77.8	2.0E-05	685349